Published in final edited form as:
Biochim Biophys Acta. 2014 September ; 1840(9): 2862–2877. doi:10.1016/j.bbagen.2014.05.002.

Intact and N- or C- terminal end truncated AQP0 function as open water channels and cell-to-cell adhesion proteins: End truncation could be a prelude for adjusting the refractive index of the lens to prevent spherical aberration

S. Sindhu Kumari[1] and **Kulandaiappan Varadaraj**[1,2,*]

[1]Department of Physiology and Biophysics, Stony Brook University, Stony Brook, NY 11794-8661, USA

[2]SUNY Eye Institute, New York, NY, USA

Abstract

Purpose—Investigate the impact of natural N- or C-terminal post-translational truncations of lens mature fiber cell Aquaporin 0 (AQP0) on water permeability (**Pw**) and cell-to-cell adhesion (**CTCA**) functions.

Methods—The following deletions/truncations were created by site-directed mutagenesis (designations in parentheses): Amino acid residues (AA) 2–6 (AQP0-N-del-2-6), AA235-263 (AQP0-1-234), AA239-263 (AQP0-1-238), AA244-263 (AQP0-1-243), AA247-263 (AQP0-1-246), AA250-263 (AQP0-1-249) and AA260-263 (AQP0-1-259). Protein expression was studied using immunostaining, fluorescent tags and organelle-specific markers. Pw was tested by expressing the respective cRNA in *Xenopus* oocytes and conducting osmotic swelling assay. CTCA was assessed by transfecting intact or mutant AQP0 into adhesion-deficient L-cells and performing cell aggregation and adhesion assays.

Results—AQP0-1-234 and AQP0-1-238 did not traffic to the plasma membrane. Trafficking of AQP0-N-del-2-6 and AQP0-1-243 was reduced causing decreased membrane Pw and CTCA. AQP0-1-246, AQP0-1-249 and AQP0-1-259 mutants trafficked properly and functioned normally. Pw and CTCA functions of the mutants were directly proportional to the respective amount of AQP0 expressed at the plasma membrane and remained comparable to those of intact AQP0 (AQP0-1-263).

Conclusion—Post-translational truncation of N- or C-terminal end amino acids does not alter the basal water permeability of AQP0 or its adhesive functions. AQP0 may play a role in adjusting the refractive index to prevent spherical aberration in the constantly growing lens.

[*]Corresponding author: Kulandaiappan Varadaraj, Department of Physiology and Biophysics, Stony Brook University, BST-6, Room # 165A; Stony Brook, NY 11794-8661, USA, Phone: (631) 444-7551; Fax: (631) 444-3432, kulandaiappan.varadaraj@stonybrook.edu.

General significance—Similar studies can be extended to other lens proteins which undergo post-translational truncations to find out how they assist the lens to maintain transparency and homeostasis for proper focusing of objects on to the retina.

1. Introduction

The crystalline lens of the human eye focuses objects near and far to the retina. For this purpose, lens transparency is critical. Lens is a unique tissue; in adult mammals it lacks innervation and is avascular with no protein turn over in the mature fiber cells. Lens comprises a monolayer of epithelial cells at the anterior region and multiple layers of fiber cells that form the bulk (Fig. 1A) which is recognized further into cortex and nucleus. The cortical region encompasses older to nascent fibers while the nuclear region houses the mature and the oldest fibers [1,2]. The incessant growth of the lens pushes the oldest fibers deep into the nuclear region (Fig. 1A); with a gradation of younger fiber cells being added upon, the youngest fiber is closer to the surface of the lens cortex.

The human lens is uniquely designed to maintain homeostasis and transparency for several decades of life to project a sharp image of objects on the retina. In order to properly focus through a process of accommodation the constantly growing lens gradually increases the refractive index of the fiber cells toward the center in a continuous gradient [3]. The refractive index of the human lens varies from ~1.386 in the less dense outer fiber cells up to ~1.406 in more dense central fiber cell layers. This refractive index gradient enhances the optical power of the lens [4]. This gradient plays an important role in reducing optical spherical aberrations of the lens [5,6].

Aquaporin (AQP) water channels and solute transporters play an important role in creating a microcirculation within the avascular lens which provides nourishment and removes metabolic wastes [7–13] in order to maintain transparency and homeostasis. AQP transmembrane channels conduct water alone, or with certain small solutes across plasma membranes depending on the osmotic gradient. Three AQPs (AQP0, AQP1 and AQP5 (Fig. 1A)) are expressed in the lens [1,14,15]. AQP1 [16] and AQP5 [15,17,18] are expressed in the epithelial cells. When new fiber cells are formed from the equatorial epithelial cells, AQP1 expression is down-regulated and replaced by AQP0 [1]. AQP0 and AQP5 are expressed in the fiber cells. AQP0 (or MIP26) is abundant in the lens fiber cells [1,9,19] constituting >44% of the total membrane protein [17]. It is expressed in both cortical and nuclear regions of the lens. The topology of AQP0 exhibits cytoplasmic N- and C-termini, five loops (two intracellular and three extracellular) and six transmembrane domains (Fig. 1B). The putative N-terminus is seven amino acid-long while the C-terminus is 43 amino acid-long and considered as a regulatory region [20–26].

During embryonic development, primary fiber cells are formed first [1]. Secondary fiber cells differentiate from the equatorial epithelial cells and form layers around the primary fiber cells. To start with, the primary and secondary fiber cells contain nucleus and other cellular organelles. However, as the fiber cells mature in the inner cortex, post-translational modifications of proteins and alterations in lipid composition ensue within these cells. Such events cause loss of fiber cell nucleus and cellular organelles [27–30] resulting in the

terminal loss of synthesis and turnover of biomolecules [27]. Lens proteins undergo age-related post-translational modifications such as deamidation, isomerization, racemization and backbone cleavage which increase as the fiber cells age [31–33].

AQP0 is synthesized as a 28 kDa protein. When the fiber cells mature, the amino (N) and/or carboxyl (C) termini of AQP0 get cleaved off as post-translational modifications. Consequently, the mature fiber cells in the inner cortex and nuclear regions of the lens harbor shorter versions of AQP0 along with the intact form. Loss of the N- and C- termini of AQP0 in mature fiber cells has been investigated and several truncation sites have been identified [32–38]. An increased rate of truncation occurs in cataractous lenses probably due to the influence of cataractogenic factors such as oxidative stress, disease condition such as hyperglycemia, natural and man-made radiation etc. [36,39–44]. Cleavage of amino acids 2–6 and 2–12 from the N-terminal end has been reported in normal lens [32,36,45,46]. Several major C-terminal end cleavage sites such as residues 228, 234, 239, 243, 245, 246, 247, 249 and 259 in human AQP0 from lens outer cortex to nuclear (core) region have been documented by mass spectrometric studies [32,33,36]. Truncation increased with progression in fiber cell age and occurred at higher levels in the lens nuclear region than in the cortex.

Several roles have been proposed for AQP0. Water channel function [9] and cell-to-cell adhesion (**CTCA**) have been reported [2,11–13,39–42,47,48]. Based on protein structural studies, distinct roles have been postulated for the intact and N- and C- terminal cleaved forms of AQP0 of the mature fiber cells [49–52]. Effect of some of the C-terminal truncations on Pw has been reported [37]. However, there is no functional *in vitro* or *in vivo* investigation on the effect of N- or C- terminal cleavage on CTCA.

In order to understand whether N- or C-terminal cleavage influences the functions of AQP0 simultaneously, we created N- or progressively shortened C- terminal truncation mutants and expressed them *in vitro* in *Xenopus* oocytes and cell culture models. Water channel and CTCA functions exhibited by the N- and C- terminal truncation mutants were studied and compared to those of intact AQP0. Our results indicate that N- and C- termini are important for protein trafficking; deletion of about 17 amino acids from the C-terminal end does not cause considerable alteration in protein trafficking or water channel and CTCA functions. N- and/or C-terminal truncations probably assist in the compact packing of mature fiber cells to reduce light diffraction and to adjust the refractive index to prevent spherical aberration in the constantly growing lens.

2. Materials and methods

2.1. Construction of plasmids encoding mouse intact (WT)-AQP0 and N/C-terminal truncation mutants

Expression constructs were generated with or without a fluorescent tag (mCherry, provided by Dr. Roger Y. Tsien, University of California, San Diego; EGFP, Clontech, Mountain View, CA) in pcDNA 3.1 myc-His vector (Invitrogen, CA) attached to the C-terminus, as described previously [49]. The vector contains CMV and T7 promoters for *Xenopus* oocyte and mammalian cell expressions. Using PCR, the coding sequence of intact (wild type)

AQP0 was amplified. The amplicon was gel purified and cloned in the vector mentioned; EGFP or mCherry tag was PCR amplified and attached to the C-terminal using restriction sites. These or untagged constructs were used for creating the N- and C-terminal deletion/truncation mutants as appropriate. Deletion/Truncation was introduced into intact AQP0 cDNA (which has a total of 263 amino acids), using QuickChange site-directed mutagenesis kit (Stratagene, La Jolla, CA) along with sense and antisense oligonucleotides specifically designed to create truncation mutants mimicking the natural truncations identified in the human lens [32–34,44]. Deletion/truncation of amino acids and the designation of the different constructs (in parentheses) were: 2–6 (AQP0-N-del-2-6), 235–263 (AQP0-1-234), 239–263 (AQP0-1-238), 244–263 (AQP0-1-243), 247–263 (AQP0-1-246), 250–263 (AQP0-1-249) and 260–263 (AQP0-1-259). Deletion/truncation points as well as the entire insert sequences were confirmed by bidirectional automated sequencing at our University Sequencing Facility. All of the mutants created are referred as truncation mutants even though the methionine at the N-terminal was retained to allow *in vitro* expression of the N-terminal mutant.

2.2. In vitro and in vivo expression and localization of AQP0

2.2.1. Pw and expression pattern of intact AQP0 and N- and C-terminal truncation mutants in Xenopus laevis oocytes—

Capped complementary RNAs (cRNAs) of intact AQP0 and N- and C-terminal truncation mutants were synthesized *in vitro* using T7 RNA polymerase (mMESSAGE mMACHINE T7 Ultra Kit, Ambion, USA), quantified using a NanoDrop spectrophotometer (ND-2000c, ThermoFisher, MA) and stored at −80°C as aliquots. Ovarian lobes were surgically removed from *Xenopus laevis* frog; stage V and VI oocytes were defolliculated using Collagenase Type II (Sigma). The oocytes were maintained at 18°C and 5 or 25 ng cRNA of the respective expression construct was injected in a volume of 25 nl/oocyte [49]. An equal volume of distilled water was injected into separate oocytes for obtaining control data.

Pw (μm/s) studies of intact AQP0 and N- or C-terminal truncation mutants were conducted in *Xenopus* oocyte heterologous system. Distilled water-injected (control) and cRNA-injected (cRNA of intact AQP0-GFP or N- or C-terminal truncation mutants of intact AQP0-EGFP) oocytes were subjected to a hypo-osmotic shock, as described previously, under normal physiological conditions of pH 7.2 and 1 mM Ca^{2+} [14,49], and the rate of swelling was recorded. We have selected the physiological conditions mentioned to mimic the prevailing conditions in the lens cortex where both intact and cleaved forms of AQP0 are present [33]).

Two days after the injections, membrane permeability assay was conducted and Pw was quantified from the initial slope of the volume change when the oocytes were subjected to an abrupt change in osmolarity from 180 to 60 mOsm (isotonic to hypotonic) at 20°C. Pw was calculated using the formula [49], $\mathrm{Pw}=\frac{(\mathrm{dV}/\mathrm{dt})}{(\mathrm{SmVw}\Delta\mathrm{c})}$, where V ($cm^3$) is the oocyte volume calculated from the cross-sectional area, S_m (cm^2) is the oocyte surface area calculated from the cross-sectional area, V_w is the molar volume of water (18 cm^3/mol) and Δ_c is the change in bath osmolarity (0.12×10^{-3} mol/cm^3).

2.2.2. Analysis of the expression pattern of intact AQP0 and N- or C-terminal truncation mutants in Xenopus laevis oocytes and quantification of the expressed proteins at the plasma membrane—Lack of a specific antibody for truncated AQP0 posed an obstacle in quantifying the amount of protein expressed at the oocyte plasma membrane. Therefore, we relied upon the EGFP tag fluorescence intensity as a measure of protein expression. Immediately following Pw measurements, eight to ten oocytes were fixed in 4% paraformaldehyde in the oocyte medium for 3hr at 22°C at room temperature. The oocytes were washed three times with oocyte medium and cryosectioned at 14 μm thickness. The sections were mounted in anti-fade Vectamount (Vector Laboratories, Inc., Burlingame, CA). Optimized Z-sectional digital images were acquired. In order to draw a parallel between protein expression at the oocyte plasma membrane and Pw, intensity of fluorescence at the plasma membrane of water-injected (control) or intact AQP0-EGFP or mutant cRNA-injected oocyte was quantified from at least six random regions of each oocyte using Sigma Scan software. Data were plotted using Sigma Plot 2000 software.

2.2.3 Expression, localization and colocalization of intact AQP0-EGFP and N- and C-terminal truncation mutant proteins in culture cells—MDCK cells from ATCC (Manassas, VA) were cultured in a 37°C incubator set with 5% CO_2. Transfections were performed using Effectene reagent (Qiagen, USA) or X-tremeGENE HP DNA transfection reagent (Roche Diagnostics, Indianapolis, IN) following the company protocols.

Endoplasmic reticulum (ER)-specific localization and plasma membrane-specific localization were tested as outlined here. MDCK cells expressing intact AQP0-EGFP and/or N- and C-terminal truncation mutants of intact AQP0-EGFP were plated onto 35 mm culture dishes containing square coverslips. These cells were transduced with ER Organelle Light Fluorescent Protein, ER-RFP (Red Fluorescent Protein; BacMam 1.0) as recommended by the manufacturer (Invitrogen) to highlight the ER. Similarly, another set of intact and truncated AQP0 was tested for plasma membrane-specific localization using CellLight® plasma membrane-RFP BacMam 2.0 reagent. After 36 hrs, cells were washed with 1xPBS, fixed with 4% paraformaldehyde and washed again with 1xPBS. The glass coverslips with cells were mounted in anti-fade Vectamount containing DAPI nuclear stain. Fluorescent signals from cells were captured separately for each experimental group using a Zeiss epifluorescent microscope fitted with EGFP and Texas Red fluorescent filters. Images of the fluorescent signals were superimposed for colocalization analysis.

Colocalization of each of the N- and C-terminal truncation mutants of intact AQP0-EGFP and intact AQP0-mCherry was also tested, as described by Varadaraj et al. [49]. In brief, MDCK cells co-transfected with the corresponding N- or C-terminal deletion mutant of intact AQP0-EGFP expression construct and intact AQP0-mCherry were grown on sterile coverslips. Fixation was performed using 4% paraformaldehyde. After washing with PBS, the coverslips containing the cells were mounted onto glass slides using anti-fade Vectamount. Forster Resonance Energy Transfer (FRET) technique was used to assess colocalization. N- and C-terminal deletion mutants with EGFP were used as donors, as appropriate (Ex 488 and Em 507) and intact AQP0-mCherry as the acceptor (Ex 587 Em 610). Imaging was performed using a Zeiss microscope containing a 63x oil immersion lens and the following filters/dichroic sets (nm): (1) EGFP cube, excitation (EX) 470/40,

emission (EM) 525/50, beamsplitter 495 (longpass); (2) Texas Red cube, excitation (EX) 545/30, emission (EM) 620/60, beamsplitter 570 (longpass) and (3) FRET cube, EX 470/40, EM 640/50, beamsplitter 495 (longpass) (Chroma Technology Corp, USA). Intact AQP0-EGFP and intact AQP0-mCherry were co-transfected and subjected to FRET analysis for the purpose of acquiring positive control FRET images.

2.2.4. Immunostaining of wild type mouse lens—Lenses from 4-month-old wild type mice were dissected out, fixed for 24 hrs in 10% neutral buffered formalin and rinsed three times in phosphate-buffered saline (PBS). Paraffin sections were cut at 4- to 6-μm thickness. Deparaffinated sections were incubated for 30 min. in 1XPBS and fixed in 4% paraformaldehyde for 30 min. Sections were incubated in 0.4% Triton X-100 in PBS for 30 min, washed with PBS, incubated overnight with anti-AQP0 antibody (Chemicon, Temecula, CA) at 4°C in a humidified chamber, washed again and exposed to FITC-conjugated IgG for 2 hours. After washing, the sections were mounted in anti-fade Vectamount (Vector Labs) containing nuclear stain DAPI. Optimized Z-sectional digital images were acquired with a Zeiss Axiovert 200 inverted microscope equipped with AxioCam and Zeiss AxioVision 4.1 software (Carl Zeiss MicroImaging, Inc.), and processed using Adobe Photoshop 7.0.

2.3. Cell-to-cell adhesion (CTCA) studies

2.3. 1. Cell aggregation assay using a rotary gyratory shaker—Cell aggregation assay was done as described [2,47]. Single cell suspensions of stably transfected L-cell (CCL-1.3; ATCC, Manassas, VA) clones expressing empty vector, AQP1, (negative controls), E-cadherin (positive control), intact AQP0 or N- and C-terminal truncation mutants of intact AQP0 were plated separately in 6-well plates pre-coated with agarose or bovine serum albumin (Sigma-Aldrich, St. Louis, MO), and rotated on a rotary gyratory shaker (80 rpm) for 30, 60 and 90 min, at 37°C. At the end of each time period, equal volume of 2% glutaraldehyde was added to stop the process. Particle number was determined using a hemocytometer. The extent of aggregation (**EA**) at various intervals was calculated from the ratio of total number of particles (single cells + number of cell-aggregates) at time 't' of incubation (N_t) to the initial number of particles (N_0) and expressed as percentage, $\mathrm{EA}(\%)=\frac{N_t}{N_0}\times 100$. As cells aggregate, the number of particles will decrease as a function of time depending on the extent of cell-to-cell adhesion exerted by each sample. The results were averaged for six experiments.

2.3.2. CTCA assay using an epifluorescent microscope—This adhesion assay is based on the novel procedure described previously from our laboratory (47,50). This assay measures semi-quantitatively the adhesion efficiency of a protein that promotes cell-to-cell adhesion. Adhesion-deficient L-cells were transfected with empty vector, AQP1, E-cadherin, intact AQP0 or N- and C-terminal truncation mutants of intact AQP0-EGFP and stably expressing colonies were selected. Cells were grown to 80% confluence and loaded with membrane permeable CellTracker™ Red CMPTX dye. Trypsinization at 21°C for 3 min was done to dissociate the cells which were subsequently neutralized, washed and counted using a Neubauer hemocytometer pre-coated with 2% BSA. The cells were suspended in serum-free Minimum Essential Medium (MEM) containing 1% BSA at a

dilution of 1×10^5 per ml. To a monolayer of 100% confluent unloaded L-cells stably expressing the respective protein in 24-well microplates, 4.5×10^4 dye-loaded cells per well (450 μl) were added and incubated for 60 min at 37°C. Cells were washed gently three times with serum-free MEM containing 1% BSA for 5 min. each, on a rotary shaker (40 rpm at room temperature). Attachment of cells to the lawn of cells depended on the adhesive property exerted by the respective sample. The cells were fixed in 2% glutaraldehyde and imaged under a Zeiss epifluorescent microscope. From each group, the number of fluorescent cells adhered to the lawn of cells was counted. E-cadherin served as a positive control. Mean and standard deviations were calculated from the values of five repetitions that used same number of cells per well under similar conditions and represented as a bar graph. Paired t-test was used to calculate the statistical significance for the difference in adhesion between two samples using the data obtained from the five experimental repeats. $P < 0.05$ was considered significant.

2.3.3. Correlation between protein expression at L-cell plasma membrane and CTCA—In order to find the correlation between the level of protein expression at L-cell plasma membrane and CTCA, 2μl of CellLight® plasma membrane-RFP BacMam 2.0 reagent per 10,000 cells was added to adhesion-deficient L-cells stably expressing EGFP-tagged intact AQP0, AQP0-N-del-2-6, AQP0-1-243, AQP0-1-246, AQP0-1-249 or AQP0-1-259 mutant plated onto coverslips and incubated for 18 hrs at 37°C. Cells were washed with PBS and fixed using 4% paraformaldehyde. After washing with PBS, the coverslips with cells were mounted onto glass slides using anti-fade Vectamount. Co-localization of plasma membrane marker and intact AQP0-EGFP or each of the mutants mentioned was studied using FRET technique. Intact AQP0-EGFP or mutant AQP0 was used as donor as appropriate (Ex 488 and Em 507) and CellLight® plasma membrane-RFP as the acceptor (Ex 587 Em 610). FRET imaging and was performed as described in sections 2.3. At least five random regions of fluorescence intensity were quantified for each sample using Sigma Scan software and plotted as a bidirectional graph using Sigma Plot 2000 software.

2.4. Statistics

Pairwise Student's t-test was performed using Sigma Plot 2000 software, Version 6.10. A value of $P < 0.05$ was considered significant.

3. Results

3.1. Functional expression of intact AQP0 and N- or C-terminal mutants

Intact (wild type) AQP0 contains 263 amino acids. Being located in the cytoplasm, the N- and C-termini of AQP0 are intracellular. The putative N- and C-termini are seven (1–7) and 43 amino acids (221–263) long, respectively (Fig. 1b).

The following truncation mutants were created (Fig. 1B); AQP0-N-del-2-6, AQP0-1-234, AQP0-1-238, AQP0-1-243, AQP0-1-246, AQP0-1-249 and AQP0-1-259. To evaluate the effects of truncation on Pw, we synthesized cRNAs *in vitro* to code for intact AQP0-EGFP and N- or C-terminal truncation mutants of intact AQP0-EGFP. We have tested and reported

previously that EGFP tag does not affect the functional characteristics (Pw and CTCA) of AQP0 under the normal physiological conditions [2,49] that exist in the human lens cortex which contains intact and N- and/or C-terminal cleaved forms of AQP0 [33]. Pw of *Xenopus* oocytes injected with distilled water, or 25 ng cRNA of intact AQP0-EGFP or N- and C-terminal mutants with EGFP were studied as given in the 'Materials and Methods' section 2.2.1. Results are shown as Table 1. Distilled water-injected oocytes served as control. Intact AQP0-EGFP injected oocytes served as positive control. Pw of oocytes injected with distilled water was 11.0 ± 3.2 μm/s while that of intact AQP0-EGFP was 43.5 ± 4.3 μm/s. Depending on the site of truncation there was variability in the level of water channel function of N- and C-terminal truncated mutants (Table 1; Fig. 2). Pw of AQP0-1-234-EGFP and AQP0-1-238-EGFP was reduced to that of water injected control. AQP0-N-del-2-6-EGFP and AQP0-1-243-EGFP showed increase in Pw compared to the water-injected control but significant decrease ($P < 0.001$) compared to intact AQP0-EGFP (Table 1; Fig. 2). C-terminal truncation mutants AQP0-1-246-EGFP, AQP0-1-249-EGFP and AQP0-1-259-EGFP showed no significant difference in Pw ($P > 0.05$) compared to intact AQP0-EGFP. It is clear that truncation at amino acid residue 238 and below significantly affected the Pw characteristic of AQP0. Truncation at amino acid residue 243 resulted in reduced Pw (36%) which is significantly less ($P < 0.001$) compared to that of intact AQP0; Pw of AQP0-1-243-EGFP was significantly more ($P < 0.001$) compared to AQP0-1-234-EGFP, AQP0-1-238-EGFP or water injected control. Truncation at residue 246 and beyond did not significantly alter Pw which remained comparable to that of intact AQP0-EGFP. It appears that absence of N-terminal residues 2–6 and C-terminal residues 221 to 245 could significantly affect the plasma membrane Pw of AQP0.

3.2. Effect of expression and plasma membrane localization of intact AQP0 and N- or C-terminal truncation mutants on plasma membrane Pw

We tested to find out whether the varied plasma membrane Pw exhibited by the mutants was influenced by the extent of expression of the respective protein at the plasma membrane. For this study, heterologous expression in *Xenopus laevis* oocytes was followed. Soon after the Pw measurements described above, oocytes were fixed and cryosectioned for protein expression and localization studies. Using an epifluorescent Zeiss confocal microscope, images were taken and scanned using SigmaScan software to quantify EGFP fluorescence intensity. As expected, there was only background fluorescence in the distilled water-injected oocytes (Fig. 3). Intact AQP0-EGFP, AQP0-N-del-2-6-EGFP, AQP0-1-243-EGFP, AQP0-1-246-EGFP, AQP0-1-249-EGFP and AQP0-1-259-EGFP localized at the oocyte plasma membrane, though with varying intensities of EGFP fluorescence. However, AQP0-1-234-EGFP and AQP0-1-238-EGFP showed intracellular localization due to impaired trafficking (Fig. 3).

Significantly low levels of plasma membrane expression and water channel permeability were observed for mutants AQP0-N-del-2-6-EGFP and AQP0-1-243-EGFP ($P < 0.001$) compared to those of intact AQP0-EGFP. However, the C-terminal truncation mutants AQP0-1-246-EGFP, AQP0-1-249-EGFP, AQP0-1-259-EGFP showed only slight reduction in the levels of protein expression at the plasma membrane compared to intact AQP0-EGFP and the reduction in Pw was not statistically significant ($P > 0.05$) indicating amino acid

residues from 247 to 263 may not be critical for protein trafficking to the plasma membrane. However, amino acid residues 221 to 245 could be involved in protein trafficking and localization since AQP0-1-243-EGFP showed significant decrease ($P<0.001$) in plasma membrane localization with majority of the protein being trapped in the cytoplasm (Fig. 3).

From the relative water channel function calculated with regard to the respective protein expression level of each of the mutants or intact AQP0-EGFP at *Xenopus* oocyte plasma membrane, it appeared that Pw was proportional to the level of protein expression at the plasma membrane (Fig. 4). Mutants with low level of protein expression at the plasma membrane (AQP0-N-del-2-6-EGFP and AQP0-1-243-EGFP) exhibited less Pw compared to those with higher levels of protein expression at the plasma membrane (AQP0-1-246-EGFP, AQP0-1-249-EGFP and AQP0-1-259-EGFP). The decrease or increase in water channel function of each mutant or intact AQP0 was relative to the level of its protein expression at the plasma membrane. Since *in vivo,* truncations occur in the proteins that are already localized at the plasma membrane and after fiber cell maturation when little or no protein turn over occurs, it can be inferred that N- and C-terminal end post-translational cleavages may not render closure of the water pore. We compared the water channel function of each mutant or intact AQP0 with its own protein expression level at the plasma membrane (with EGFP fluorescence as a measure) and not between mutant and intact AQP0 directly because in the C-terminal mutants, the EGFP fluorescent protein folding may vary. However, the current study shows that the N- and C-terminal truncated AQP0 channels transport water and the water channel function is proportional to the level of protein expression at the plasma membrane.

3.3. Expression and localization of intact AQP0 and N- and C-terminal truncation mutants in culture cells

For proper functioning, the N- and C-terminal mutants of intact AQP0 must first traffic and reach the plasma membrane without interruption. To further confirm our results, we used heterologous cell culture expression system to test for trafficking and localization. Since AQP0-1-234 and AQP0-1-238 mutants did not traffic to the membrane when expressed in *Xenopus* oocytes, these two mutants were excluded from the study. The following experiment was designed to test whether each of the mutant proteins (AQP0-N-del-2-6, AQP0-1-243, AQP0-1-246, AQP0-1-249 and AQP0-1-259) traffic through endoplasmic reticulum (ER) and localize at the plasma membrane. To locate the presence of the protein in the ER, Organelle Light ER-RFP marker was used. MDCK cells expressing intact or mutant AQP0 with EGFP were plated separately on coverslips and transduced with Organelle Light ER-RFP marker. The coexpressing cells were viewed under EGFP filter in an epifluorescence microscope to image green fluorescence corresponding to EGFP-tag in intact AQP0/mutant AQP0 protein or viewed under Texas Red filter to image Organelle Light ER-RFP marker protein. Merging of the respective EGFP and ER-RFP images exhibited yellow color indicating colocalization of the ER marker protein and intact or mutant AQP0 protein (Fig. 5). The green signal due to the EGFP tag visible mostly at the periphery of the merged images indicated plasma membrane localization of the respective protein (Fig. 5). The blue spots represent cell nuclei stained with DAPI. This experiment showed that the tested mutants of AQP0-EGFP followed the ER trafficking pathway and

localized at the plasma membrane like the intact AQP0. Low levels of membrane localization were observed for AQP0-N-del-2-6 and AQP0-1-243. Similar to intact AQP0, AQP0-1-246, AQP0-1-249 and AQP0-1-259 proteins localized mostly at the plasma membrane.

Coexpression of intact AQP0 or mutant AQP0 (AQP0-N-del-2-6-EGFP, AQP0-1-243-EGFP, AQP0-1-246-EGFP, AQP0-1-249-EGFP and AQP0-1-259-EGFP) and membrane marker CellLight® plasma membrane-RFP was tested in culture cells. MDCK cells stably expressing intact AQP0-EGFP or C-terminal truncation mutant AQP0-1-243-EGFP grown on coverslips were transduced with plasma membrane marker CellLight® plasma membrane-RFP. Intact AQP0-EGFP and mutant AQP0-EGFP chimeric proteins coexpressed at the plasma membrane, with differing degrees of intensity. Images of intact AQP0-EGFP or mutants (AQP0-N-del-2-6-EGFP, AQP0-1-243-EGFP, AQP0-1-246-EGFP, AQP0-1-249-EGFP and AQP0-1-259-EGFP), and CellLight® plasma membrane-RFP, taken of the same cell, were superimposed to verify colocalization. The emerged yellow signal indicated colocalization of the intact or mutant AQP0 with CellLight® plasma membrane-RFP at the plasma membrane. We have shown images of colocalization for only intact AQP0 and the C-terminal mutant AQP0-1-243-EGFP (Fig. 6A). The blue spots in the Figure 6A are DAPI-stained cell nuclei. Decreased levels of yellow signals for AQP0-N-del-2-6-EGFP (image not shown) and AQP0-1-243-EGFP compared to intact AQP0-EGFP have indicated low levels of mutant AQP0 protein localization at the plasma membrane. However, other C-terminal truncation mutants AQP0-1-246-EGFP, AQP0-1-249-EGFP and AQP0-1-259-EGFP displayed plasma membrane localization (data not shown) comparable to that of intact AQP0.

After synthesis, aquaporin proteins are assembled into tetramers in the ER before trafficking to the plasma membrane for insertion [51,52]. To test the possibility whether the intact and N- and C-terminal truncation mutants of AQP0 could exist at the membrane as tetramer complex *in vivo*, we coexpressed each of the truncation mutant of AQP0 (AQP0-N-del-2-6-EGFP, AQP0-1-234-EGFP, AQP0-1-238-EGFP, AQP0-1-243-EGFP, AQP0-1-246-EGFP, AQP0-1-249-EGFP and AQP0-1-259-EGFP) and intact AQP0-EGFP into MDCK cells and subjected to FRET analysis; EGFP was the donor fluorophore and mCherry was the acceptor (Fig. 6B a–x). MDCK cells cotransfected with intact AQP0-mCherry and intact AQP0-EGFP and subjected to FRET analysis served as positive control (Fig. 6B a–c). In the experimental groups, FRET signal indicated colocalization of intact AQP0 and mutant proteins as heterotetramers within 100Å for AQP0-N-del-2-6, AQP0-1-243, AQP0-1-246, AQP0-1-249 and AQP0-1-259 (Fig. 6B d–f, m–o, p–r, s–u, v–x respectively). However, AQP0-1-234 and AQP0-1-238 were negative to FRET signal (Fig. 6B g–i and j–l respectively) confirming lack of membrane localization due to interruption in protein trafficking. Decreased levels of FRET signals for AQP0-N-del-2-6-EGFP and AQP0-1-243-EGFP (Fig. 6 B d–f and m–o) compared to intact AQP0-EGFP and other C-terminal truncation mutants (AQP0-1-246, AQP0-1-249 and AQP0-1-259) indicate low levels of protein localization of these mutants at the plasma membrane.

3.4. Cell-to-cell adhesion (CTCA) studies

Based on the protein expression and functional studies on *Xenopus* oocytes, only the following truncation mutants AQP0-N-del-2-6, AQP0-1-243, AQP0-1-246, AQP0-1-249 and AQP0-1-259 that trafficked to the plasma membrane and formed functional water channels (section 3.1) were selected for CTCA studies.

Mouse L-fibroblast cells lacking endogenous cell adhesion molecules were stably transfected with untagged vector (negative control), AQP1 (negative control), E-cadherin (positive control), intact AQP0 or N- and C- terminal truncation mutants (AQP0-N-del-2-6, AQP0-1-243, AQP0-1-246, AQP0-1-249 and AQP0-1-259) separately and individual clones were selected using G418. First, the cell-to-cell adhesive property was tested using cell aggregation assay in a rotary gyratory shaker. The tested mutants displayed different levels of cell aggregation as a function of time (Fig. 7) consequently reducing the number of non-aggregating individual L-cells. E-cadherin served as a positive control [47,53] and was used as a standard to calculate the relative aggregation by other proteins. Cells transfected with AQP0-1-246, AQP0-1-249 and AQP0-1-259 showed no significant ($P > 0.05$) difference in cell aggregation compared to those transfected with intact AQP0 (Fig. 7). However, cells transfected with AQP0-N-del-2-6 and AQP0-1-243 showed less aggregation compared to those transfected with intact AQP0. The extent of aggregation exhibited by the different proteins can be summarized as follows: intact AQP0 = AQP0-1-259 = AQP0-1-249 = AQP0-1-246 > AQP0-N-del-2-6 = AQP0-1-243 (Fig. 7). As expected, empty vector or AQP1 did not show considerable aggregation indicating the absence of CTCA capability. Similar result for AQP1 had also been observed by Hiroaki et al. [54] and Kumari and Varadaraj [47].

Intact AQP0, truncation mutants and the controls tested above were subjected to a novel fluorescent assay developed previously by our laboratory [47]. Mouse fibroblast L-cells stably expressing empty vector, negative control AQP1, positive control E-cadherin, intact AQP0, N- and C- terminal deletion/truncation mutants, AQP0-N-del-2-6, AQP0-1-243, AQP0-1-246, AQP0-1-249 and AQP0-1-259 grown to confluence were subjected to this assay. Compared to negative controls, namely, L-cells expressing empty vector or AQP1 (Fig. 8A, a,b), CTCA induced by intact AQP0 and N- and C- terminal mutants AQP0-N-del-2-6, AQP0-1-243, AQP0-1-246, AQP0-1-249 and AQP0-1-259 expressing cells was statistically significant ($P < 0.001$; Fig. 8A e–i; B). Compared to the positive control L-cells expressing E-cadherin (Fig. 8A, c; B), CTCA efficiency of L-cells expressing intact AQP0 and N- and C- terminal truncation mutants (Fig. 8A e–i; B) was significantly less ($P < 0.001$). Cells transfected with AQP0-1-246, AQP0-1-249 and AQP0-1-259 showed no significant difference ($P > 0.05$) in CTCA compared to those expressing intact AQP0 (Fig. 8B). However, AQP0-N-del-2-6 and AQP0-1-243 showed less CTCA compared to cells expressing intact AQP0 ($P<0.01$). Same trend was noticed for these mutants with regard to water channel function (Section 3.1; Fig. 2). The reduction in CTCA of AQP0-N-del-2-6 ($P < 0.001$) and AQP0-1-243 ($P < 0.001$) was statistically significant compared to the C-terminal truncation mutants AQP0-1-246, AQP0-1-249 and AQP0-1-259 or intact AQP0.

To find out the reason for the reduction in CTCA observed for AQP0-N-del-2-6 and AQP0-1-243, we examined the correlation between CTCA and protein expression at the plasma membrane of L-cells. Data obtained showed that the trend for CTCA of AQP0-N-del-2-6 or AQP0-1-243 was very similar to that of intact AQP0 (Fig. 8C) considering the level of protein expression at the plasma membrane. More cells adhered when there was more mutant AQP0 protein available at the plasma membrane as in intact AQP0, AQP0-1-246, AQP0-1-249 and AQP0-1-259. Data collected showed a trend similar to that obtained from water channel permeability studies described in sections 3.1 and 3.2. For equal amounts of cRNA injected into the *Xenopus* oocytes, the plasma membrane Pw of AQP0-N-del-2-6 and AQP0-1-243 was significantly less than that of the intact AQP0. However, when the correlation between water channel function and protein expression level at the plasma membrane was analyzed, water channel permeability of AQP0-N-del-2-6 and AQP0-1-243 was comparable to that of intact AQP0 (Fig. 4). In summary, results of the *in vitro* studies on water channel and CTCA functions of intact AQP0 and N/C-terminal truncation mutants that mimicked the natural post-translational cleavages of AQP0 *in vivo* in the mature fiber cells of the mammalian lens, followed a comparable trend (Figs. 4, 8C).

4. Discussion

In normal human lens, intact and truncated AQP0 proteins are present in the inner cortical and outer nuclear regions [32,33,36,37]. In the current study, Co-expression of N- or C-terminal truncation mutant and intact AQP0 in MDCK cells showed colocalization at the plasma membrane (Fig. 6A d–f). In vivo, N- and C- terminal post-translational modifications take place after intact AQP0 had trafficked and localized at the plasma membrane. This event cannot be reproduced *in vitro* using the existing cell culture models. Also, there are no specific proteases currently available to create truncations that could mimic the natural post-translational modifications observed in human lens. However, *in vitro* studies like the current investigation can provide clues for what might be happening in the lens.

AQP0-N-del-2-6, AQP0-1-234, AQP0-1-238 and AQP0-1-243 truncation mutants were totally or partially inhibited from trafficking to the plasma membrane depending on the site of truncation (Fig. 3). AQP0-1-234 and AQP0-1-238 were unable to traffic to the plasma membrane, consequently causing no increase in plasma membrane Pw which remained the same as that of water-injected control oocytes (Fig. 2). AQP0-N-del-2-6 and AQP0-1-243 showed decrease in plasma membrane localization and therefore caused 49% and 36% reduction in Pw, respectively compared to intact AQP0. Calibration of relative plasma membrane Pw based on the fluorescence intensity of the EGFP tag of the respective truncation mutant or intact AQP0 at oocyte plasma membrane, AQP0-N-del-2-6 and AQP0-1-243 showed a proportional correlation between fluorescence intensity and Pw. Reduction in protein expression at the plasma membrane has been observed for the bovine mutants AQP0-1-228 [55] and AQP0-1-225 [20], and human mutant AQP0 [37] in expression studies using *Xenopus* oocytes. Current and previous investigations suggest that the N- and C-termini of the AQP0 are critical for normal trafficking and membrane localization. It has also been shown that water channel function of AQP0 is regulated by calcium-calmodulin and phosphorylation at the proximal C-terminal domain [21–25].

The created C-terminal truncation mutants namely, AQP0-1-246, AQP0-1-249 and AQP0-1-259 resembling the natural truncations in human lens [32,33,36] were fully functional under the tested normal physiological conditions that exist in the lens cortex where intact and N- and/or C-terminal cleaved AQP0 are present [33]. AQP0-N-del-2-6, AQP0-1-243, AQP0-1-246, AQP0-1-249 and AQP0-1-259 cleaved forms and intact AQP0 that gave positive results for Pw were tested for CTCA in adhesion-deficient mouse fibroblast L-cells. Under normal physiological conditions, all of them promoted CTCA, although with varied efficiencies. We and others have previously reported the adhesion capability of intact AQP0 [2,20-26,47,48,50]. AQP0-N-del-2-6 and AQP0-1-243 showed decrease in CTCA by 52% and 46%, respectively, compared to the adhesion property exhibited by intact AQP0. However, considering the CTCA exerted by intact AQP0 based on the level of its plasma membrane localization, AQP0-N-del-2-6 and AQP0-1-243 showed that the reduction in CTCA was a reflection of the decrease in the amount of protein expressed at the plasma membrane. CTCA function of AQP0-1-246, AQP0-1-249 and AQP0-1-259 demonstrated no significant change (Fig. 7, 8B) compared to that of intact AQP0. Post-translational truncation at the N- and C-termini is not unique to AQP0 and had been observed for other lens proteins also. Accumulation of N- and C-terminal cleavages without affecting lens transparency has been identified for crystallin [56–58], connexins (Cx50 [59–61] and Cx46 [62]) and beaded filaments [63] of the mature fiber cells. C-terminal post-translational cleavages were present in human lens as early as 2–years of age [36] suggesting AQP0 truncation is a normal fiber cell-maturation-related event. Our current and previous investigations [2,15,47] suggest that N- or C-terminal truncated AQP0 continue to function as water channels and CTCA protein during fiber cell maturation and aging processes. It appears that truncations of N- and C-terminal ends of AQP0 are natural events in the fiber cell maturation and compaction process. Truncation could be a mechanism to conveniently pack the older fiber cells compactly in a place where there is no natural protein turnover, to aid in adjusting the refractive index and preventing spherical aberration of the continuously growing lens.

Conflicting views exist in literature regarding the function/s of intact and end cleaved forms of AQP0. Electron diffraction microscopy studies indicate that intact AQP0 functions as an open water channel but not as an adhesion protein and C-terminal-cleaved AQP0 functions as an adhesion protein but is closed as a water pore [64,65]. X-ray crystallographic analyses [66] and molecular dynamic studies [67] suggest that intact AQP0 is an open water channel and may also participate in CTCA. *In vitro* liposome experiments by Michea et al. [68,69] indicate that intact AQP0 may participate in CTCA. Their results show that AQP0 adheres to negatively charged membrane vesicles, indicating the electrostatic nature of adhesion. It has been suggested that the extracellular loops of AQP0 interact with the lipids of the opposing plasma membrane [66–71]. We have shown previously that intact AQP0 is capable of providing CTCA in addition to being a water channel [2,15,47]. Our current results show that N- or C-Terminal cleaved forms can conduct water as well as provide CTCA.

Immunostaining of lens cross sections using an anti-AQP0 antibody raised against a C-terminal peptide indicates the natural post-translational truncation of AQP0. Figure 9A shows differential staining; the outer cortical fiber cells bind the antibody intensely while the

intensity of binding decreases toward the inner cortex and is almost absent in the nuclear region. Since the antibody is raised against a peptide (amino acids: 247th-263rd) from the C-terminal end of AQP0, the reduced antibody binding in the inner cortex and lack of binding in most of the nuclear regions could be due to the loss of the C-terminal end by natural truncation [32,33]. Figure Fig 9A(a–c) shows the gradual decrease in antibody binding from cortex to the nucleus. Dehydration and compaction of the fiber cells might also have rendered the epitopes inaccessible to the antibody. A diffusion barrier region which restricts the passage of solutes and water from the cortical region into the nucleus has been recognized by several studies [72–74].

Several junctions are present in the fiber cell plasma membrane depending on the area of the lens for maintaining membrane integrity and/or cell-to-cell communication to adjust the refractive index as well as to maintain transparency and homeostasis. In the outer cortex, fiber cells have N-cadherin adhesion junctions (extracellular width, 20–40 nm), connexin (Cx46 and Cx50) gap junctions (16–17 nm) and small patches of intact AQP0 square array thin junctions (11–13 nm). Within the lens outer cortex, AQP0 square arrays appear as 6.6 nm repeats [70,71,75,76]. Level of N-cadherin which is critical in lens differentiation and maintenance [77–81] is present at reduced levels in the inner cortex and is absent in the lens nucleus and adhesion junctions are coincidently reduced or absent [82]; however, inner cortex and nucleus contain gap junctions formed by connexins (16–17 nm) and thin junctions by AQP0 (11–13 nm) [11–13,39–42,70,71,83]. Cell membranes have specialized AQP0-lipid interactions that determine the fiber cell shape, surface topology and size of the intercellular junctions [84]. Large patches of AQP0 square arrays pair with the protein-free lipid membrane bilayers to develop new and asymmetric thin junctions; pairing of 7 nm thick AQP0 square arrays with 4–5 nm thick lipid bilayers produces narrow junctions of about 11 nm [70,71,85,86].

Thin junctions formed by AQP0 between fiber cell membranes could play a significant role in the compact packing of the fiber cells. Since lens is continuously growing peripherally, compact packing is necessary to adjust and maintain a refractive index gradient which should be low in the cortex and high in the nucleus; otherwise spherical aberration will result in improper focusing. As the fiber cells in the inner cortex mature they lose the cellular nucleus and organelles [27,87] probably to reduce light diffraction and to aid in fiber cell compaction [88–90]. Even though many studies exist on fiber cell architectural changes and post-translational cleavage of lens proteins, the physiological significance of these processes has not been addressed satisfactorily. Based on our current and previously published data (2,47,48] and from relevant literature, we hypothesize that intact and post-translationally N- and C-terminal cleaved AQP0 play a significant role in fiber cell compaction and refractive index adjustment by regulating the extracellular space between fiber cells by providing firm CTCA and carrying out fiber cell dehydration. Our interpretations are depicted as schematic models through Figures 9B, C and D that explain how AQP0 could be playing a significant role in fiber cell compaction, probably to aid in adjusting the refractive index of the lens. We speculate that for proper compaction of the fiber cells, deletion of cytoplasmic N- and C-terminal ends of membrane proteins like AQP0 which interact with other proteins may be necessary; these end cleavages correlate well with fiber cell rearrangements and remodeling (Fig. 9B) from a smooth hexagonal appearance in

the outer cortex to an interdigitated and irregular cross-sectional appearance in the inner cortex followed by an irregular undulating membrane cross-sectional appearance in the nucleus [90]. Normally in the outer cortex fiber cells, the N- and C-terminal ends of intact AQP0 interact with cytoskeletal proteins such as actins [91] and beaded filaments [92,93] and get uniformly distributed throughout the plasma membrane, except a few areas (e.g., with small patches of square arrays), giving an ordered hexagonal architecture [76]. Lens cytoskeletal proteins control the shape of fiber cells [90,94–96]. *In vivo* and *in vitro* studies have shown the interactions of lens membrane proteins and cytoplasmic proteins [91,96–100]. The remarkable cellular rearrangements that occur in the mature fiber cells in the inner cortex and nucleus most probably could be due to dissociation of cytoplasmic N- and C-terminal ends of membrane proteins like AQP0, connexins etc., from the cytosolic proteins like crystallins and lens-specific cytoskeletal beaded filament proteins such as filensin and CP49. In order to adjust the refractive index and reduce diffraction of light in the ocular lens, fiber cells undergo a unique process of maturation by losing their nuclei as well as eliminating cellular organelles and cytoskeletal proteins; actins, intermediate filaments and beaded filaments filensin and CP49 are absent in the lens nucleus [90–106]. Blankenship et al. [105] showed that filensin rod domain and phakinin (CP49) localized at the membrane lining region in outer cortex cells and to the central region of the cytoplasm in inner cortex cells. Similar observations were also recorded in rat lens [107]. Light-scattering was observed in the lenses of filensin and CP49 knockout mice starting very early in life [108–110]. This could be due to failure in AQP0 distribution and the consequent lack of CTCA in the cortex leading to abnormalities in refractive index adjustment. During fiber cell maturation in the inner cortex and outer nucleus, interaction of AQP0 with cytoskeletal proteins, crystallins and other cytosolic proteins which help in the membrane distribution of AQP0 become progressively lost due to the gradual elimination of the N- and C- terminal ends of AQP0 [33]. Loss of AQP0 N- and C-terminal ends promotes migration [111] and aggregation of AQP0 into large square arrays [68,76] without the constraint of being tethered to other proteins and subsequent formation of collective thin junctions (Fig. 9C) due to possible intermolecular attraction between tetramers and lipids [112]; AQP0 reorganizes in order to minimize the surface energy to become stable in the inner cortex and nucleus by pushing the connexin gap junction plaques to the edge of the large square arrays as shown by atomic force microscopy studies [11–13,39–42]. We postulate that, first AQP0 N- and C-terminal end cleavages occur, followed by development of large patches of square arrays that form thin junctions to reduce the extracellular space and water content.

Gradual reduction in the extracellular space and water content (water has low refractive index) between the mature fiber cells of the inner cortex and nucleus, and dehydration in the cytoplasm have been observed [71]. We speculate that this strategy could be to increase the refractive index of the lens core for proper focusing of objects on to the retina. Korlimbinis et al. [33] have shown that in human lens, accumulation of N- and C-terminal end cleaved AQP0 is a gradual process and it starts from the fiber cells in the inner cortex; the percentage of N- and C-terminal end cleaved AQP0 increases toward the core of lens nucleus (gradual reduction in antibody binding, Fig. 9A(c). This increase in N- and C-terminal end cleaved AQP0 coincides with the reduction in the extracellular space and fiber cell compaction [90]. Posttranslational modifications in the water soluble crystallins might

have promoted crystallin hydrophobicity and thus might have enabled the fiber cells to lose water from the cytoplasm in the inner cortex and nucleus to increase the refractive index. Stratified syncytia formed by the fusion of several central nuclear fibers [113] might have also facilitated dehydration to adjust the refractive index gradient in the lens. Loss of water from the cytoplasm might have promoted fiber cell compaction. N- and C-terminal end cleaved AQP0 in the square arrays might have facilitated removal of water from extracellular space because our *in vitro* oocyte expression studies showed that the N- and C-terminal end cleaved forms of AQP0 are capable of functioning as water channels (Fig. 2,3; also, [37]). Low pH and high calcium in the inner cortex and nucleus of the lens also enhance AQP0 water channel efficiency [14,21,22]. The steady increase in N- and C-terminal end cleaved AQP0 as well as the gradual reduction in extracellular space and water content of the fiber cells may assist in maintaining the most conducive refractive index to focus objects on to the retina in the constantly growing lens.

Several investigators have reported the presence of a diffusion barrier at the interface of the inner cortex and nucleus of the lens (Fig. 9D) that does not allow free movement of solutes (e.g., antioxidant glutathione) and water deep into the nucleus [72,73]. However, the possible purpose or the mechanism behind this lens barrier development in the inner cortex [74] remains unknown. Based on our present and previously published data (2,15,47] as well as inferring from reports on observations by other investigators [70,71,75–77,79,83–85,106,120], we hypothesize the following: The constantly growing lens has to adjust and maintain the increasing refractive index gradient, from the cortex to the nucleus, for proper focusing. To increase the refractive index, a gradual reduction in the extracellular space as well as removal of water content from both the extracellular space and cytoplasm of the mature fiber cells occur in the inner cortex and nucleus. N- and/or C-terminal end cleavage in AQP0, beaded filaments and crystallins [114] aid the process. N- and/or C-terminal cleavages and the establishment of large patches of square arrays of AQP0 that form thin junctions help to reduce extracellular space between fiber cells; similar cleavages in crystallins increase the its hydrophobic fraction [114] and could promote fiber cell dehydration leading to outward flow of free water and solutes towards the inner cortex from the nucleus (Fig. 9D). The microcirculation model put forth by Mathias et al. [8] which is based on the distribution of ion pumps, transporters, gap junctions and AQP0 states that a standing circulating current created by the lens enters at both poles and exits at the equator after passing into and through the fiber cells; a flow of water through aquaporins is generated by the circulating flux of ions and the flow is from outer cortex toward the inner cortex. We propose that there could be an outward flow of solutes and water from the nuclear and inner cortical regions (Fig. 9D). This outward flow of solutes and water due to fiber cell dehydration and extracellular space reduction possibly meet the exit route of the solutes and water from the outer cortex proposed in the model by Mathias et al. [8]. This area of merging could create a resistance zone and most probably, develop into and exist as a diffusion barrier preventing solutes and water from the outer cortex to move towards the center of the lens where dehydration takes the priority. As shown in Figure 9D, we postulate that the water content coming out from the nuclear regions and inner cortex join the outflow of solutes and water from the cortical region and exit at the equator as shown by Mathias et al. [8].

To summarize, our results show that N- and C-termini of AQP0 are important for protein trafficking. Two of the truncation mutants AQP0-1-234 and AQP0-1-238 did not traffic to the plasma membrane. AQP0-N-del-2-6 and AQP0-1-243 showed decrease in protein expression at the plasma membrane. Presence of a specific length of the proximal C-terminus, containing amino acids as trafficking signal, seems to be necessary for normal trafficking to the plasma membrane. This could be the reason why *in vivo* N- and C-terminal processing takes place after the protein has reached the plasma membrane. Our data also suggest that loss of N and/or C-terminal ends of AQP0 is required for fiber cell compaction process which is caused by reducing the extracellular space and water to adjust the refractive index of the constantly growing lens for preventing spherical aberration while focusing.

In conclusion, our studies show that both intact and N- and/or C-termini posttranslationally truncated AQP0 function as open water channels and promote CTCA under normal physiological conditions. The reduction in the length of N- and C-termini could be a consequence of fiber cell maturation and aging, and a strategy for compact packing of the cytosolic proteins as well as rearranging of the membrane proteins in the fiber cells. This process helps to reduce light diffraction and facilitates adjustment of the refractive index to prevent spherical aberration of the continually growing lens for proper focusing.

Acknowledgments

This work was supported by NIH-NEI grant R01: EY20506.

References

1. Varadaraj K, Kumari S, Mathias RT. Functional expression of aquaporins in embryonic, postnatal, and adult mouse lenses. Dev Dyn. 2007; 236:1319–1328. [PubMed: 17377981]
2. Varadaraj K, Kumari SS, Mathias RT. Transgenic expression of AQP1 in the fiber cells of AQP0 knockout mouse: effects on lens transparency. Exp Eye Res. 2010; 91:393–404. [PubMed: 20599966]
3. Banh A, Bantseev V, Choh V, Moran KL, Sivak JG. (2006) The lens of the eye as a focusing device and its response to stress. Prog Retin Eye Res. 2006; 25:189–206. [PubMed: 16330238]
4. Eugene, H. Optics. 2. Addison Wesley; 1987. p. 178
5. Mostafapour MK, Schwartz CA. Age-related changes in the protein concentration gradient and the crystallin polypeptides of the lens. Invest Ophthalmol Vis Sci. 1982; 22:606–612. [PubMed: 7076406]
6. Sivak, JG. Optical variability of the fish lens. In: Douglas, RH.; Djamgoz, MBA., editors. The Visual System of Fish. Chapman & Hall; London: 1990. p. 63-80.
7. Robinson KR, Patterson JW. Localization of steady currents in the lens. Curr Eye Res. 1983; 2:843–847. [PubMed: 7187641]
8. Mathias RT, Rae JL, Baldo GJ. Physiological properties of the normal lens. Physiol Rev. 1997; 77:21–50. [PubMed: 9016299]
9. Varadaraj K, Kushmerick C, Baldo GJ, Bassnett S, Shiels A, Mathias RT. The role of MIP in lens fiber cell membrane transport. J Membr Biol. 1999; 170:191–203. [PubMed: 10441663]
10. Kumari SS, Varadaraj K. Aquaporin 5 knockout mouse lens develops hyperglycemic cataract. Biochem Biophys Res Commun. 2013; 441:333–338. [PubMed: 24148248]
11. Buzhynskyy N, Girmens JF, Faigle W, Scheuring S. Human cataract lens membrane at subnanometer resolution. J Mol Biol. 2007a; 374:162–169. [PubMed: 17920625]
12. Buzhynskyy N, Hit RK, Walz T, Scheuring S. The supramolecular architecture of junctional microdomains in native lens membranes. EMBO Rep. 2007b; 8:51–55. [PubMed: 17124511]

13. Scheuring S, Buzhynskyy N, Jaroslawski S, Gonçalves RP, Hite RK, Walz T. Structural models of the supramolecular organization of AQP0 and connexons in junctional microdomains. J Struct Biol. 2007; 160:385–394. [PubMed: 17869130]
14. Varadaraj K, Kumari S, Shiels A, Mathias RT. Regulation of aquaporin water permeability in the lens. Invest Ophthalmol Vis Sci. 2005; 46:1393–1402. [PubMed: 15790907]
15. Kumari SS, Varadaraj M, Yerramilli VS, Menon AG, Varadaraj K. Spatial expression of aquaporin 5 in mammalian cornea and lens, and regulation of its localization by phosphokinase A. Mol Vis. 2012; 18:957–967. [PubMed: 22550388]
16. Hamann S, Zeuthen T, La Cour M, Ottersen OP, Agre P, Nielsen S. Aquaporins in complex tissues: distribution of aquaporins 1–5 in human and rat eye. Am J Physiol. 1998; 274:C1332–C1345. [PubMed: 9612221]
17. Bassnett S, Wilmarth PA, David LL. The membrane proteome of the mouse lens fiber cell. Mol Vis. 2009; 15:2448–2463. [PubMed: 19956408]
18. Grey AC, Walker KL, Petrova RS, Han J, Wilmarth PA, David LL, Donaldson PJ, Schey KL. Verification and spatial localization of aquaporin-5 in the ocular lens. Exp Eye Res. 2013; 108:94–102. [PubMed: 23313152]
19. Shiels A, Bassnett S, Varadaraj K, Mathias RT, Al-Ghoul K, Kuszak J, Donoviel D, Lilleberg S, Friedrich G, Zambrowicz B. Optical dysfunction of the crystalline lens in aquaporin-0-deficient mice. Physiol Genomics. 2001; 7:179–186. [PubMed: 11773604]
20. Varadaraj K, Kumari SS, Mathias RT. Lens Major Intrinsic Protein vesicle trafficking requires a sorting signal. Invest Ophthalmol Vis Sci. 2000; 41:S864.
21. Németh-Cahalan KL, Kalman K, Hall JE. Molecular basis of pH and Ca^{2+} regulation of aquaporin water permeability. J Gen Physiol. 2004; 123:573–580. [PubMed: 15078916]
22. Kalman K, Németh-Cahalan KL, Froger A, Hall JE. AQP0-LTR of the *Cat*^{Fr} mouse alters water permeability and calcium regulation of wild type AQP0. Biochim Biophys Acta. 2006; 1758:1094–1099. [PubMed: 16515771]
23. Kalman K, Németh-Cahalan KL, Froger A, Hall JE. Phosphorylation determines the calmodulin-mediated Ca^{2+} response and water permeability of AQP0. J Biol Chem. 2008; 283:21278–21283. [PubMed: 18508773]
24. Gold MG, Reichow SL, O'Neill SE, Weisbrod CR, Langeberg LK, Bruce JE, Gonen T, Scott JD. AKAP2 anchors PKA with aquaporin-0 to support ocular lens transparency. EMBO Mol Med. 2012; 4:15–26. [PubMed: 22095752]
25. Reichow SL, Clemens DM, Freites JA, Németh-Cahalan KL, Heyden M, Tobias DJ, Hall JE, Gonen T. Allosteric mechanism of water-channel gating by Ca^{2+}-calmodulin. Nat Struct Mol Biol. 2013; 20:1085–1092. [PubMed: 23893133]
26. Liu J, Xu J, Gu S, Nicholson BJ, Jiang JX. Aquaporin 0 enhances gap junction coupling via its cell adhesion function and interaction with connexin 50. J Cell Sci. 2011; 124:198–206. [PubMed: 21172802]
27. Bassnett S, Beebe DC. Coincident loss of mitochondria and nuclei during lens fiber cell differentiation. Dev Dyn. 1992; 194:85–93. [PubMed: 1421526]
28. Vrensen GF, Graw J, De Wolf A. Nuclear breakdown during terminal differentiation of primary lens fibres in mice: a transmission electron microscopic study. Exp Eye Res. 1991; 52:647–659. [PubMed: 1855541]
29. Borchman D, Yappert MC. Lipids and the ocular lens. J Lipid Res. 2010; 51:2473–2488. [PubMed: 20407021]
30. Wride MA. Lens fibre cell differentiation and organelle loss: many paths lead to clarity. Philos Trans R Soc Lond B Biol Sci. 2011; 366:1219–1233. [PubMed: 21402582]
31. Han J, Schey KL. Proteolysis and mass spectrometric analysis of an integral membrane: aquaporin 0. J Proteome Res. 2004; 3:807–812. [PubMed: 15359735]
32. Ball LE, Garland DL, Crouch RK, Schey KL. Post-translational modifications of aquaporin 0 (AQP0) in the normal human lens: spatial and temporal occurrence. Biochemistry. 2004; 43:9856–9865. [PubMed: 15274640]

33. Korlimbinis A, Berry Y, Thibault D, Schey KL, Truscott RJ. Protein aging: truncation of aquaporin 0 in human lens regions is a continuous age-dependent process. Exp Eye Res. 2009; 88:966–973. [PubMed: 19135052]
34. Horwitz J, Robertson N, Wong M, Zigler J, Kinoshita J. Some properties of lens plasma membrane polypeptides isolated from normal human lenses. Exp Eye Res. 1979; 28:359–365. [PubMed: 436982]
35. Takemoto L, Takehana M, Horwitz J. Covalent changes in MIP26K during aging of the human lens membrane. Invest Ophthalmol Vis Sci. 1986; 27:443–446. [PubMed: 3949474]
36. Schey KL, Little M, Fowler JG, Crouch RK. Characterization of human lens major intrinsic protein structure. Invest Ophthalmol Vis Sci. 2000; 41:175–182. [PubMed: 10634618]
37. Ball LE, Little M, Nowak MW, Garland DL, Crouch RK, Schey KL. Water permeability of C-terminally truncated aquaporin 0 AQP0 1-243 observed in the aging human lens. Invest Ophthalmol Vis Sci. 2003; 44:4820–4828. [PubMed: 14578404]
38. Gutierrez DB, Garland D, Schey KL. Spatial analysis of human lens aquaporin-0 post-translational modifications by MALDI mass spectrometry tissue profiling. Exp Eye Res. 2011; 93:912–920. [PubMed: 22036630]
39. Mangenot S, Buzhynskyy N, Girmens JF, Scheuring S. Malformation of junctional microdomains in cataract lens membranes from a type II diabetes patient. Pflugers Arch. 2009; 457:1265–1274. [PubMed: 19034495]
40. Buzhynskyy N, Sens P, Behar-Cohen F, Scheuring S. Eye lens membrane junctional microdomains: a comparison between healthy and pathological cases. New J Phys. 2011; 13:085016.
41. Colom A, Casuso I, Boudier T, Scheuring S. High-speed atomic force microscopy: cooperative adhesion and dynamic equilibrium of junctional microdomain membrane proteins. J Mol Biol. 2012; 423:249–256. [PubMed: 22796628]
42. Rico F, Picas L, Colom A, Buzhynskyy N, Scheuring S. The mechanics of membrane proteins is a signature of biological function. Soft Matter. 2013; 9:7866–7873.
43. Takemoto L, Smith J, Kodama T. Major intrinsic polypeptide (MIP26K) of the lens membrane: covalent change in an internal sequence during human senile cataractogenesis. Biochem Biophys Res Commun. 1987; 142:761–766. [PubMed: 3827901]
44. Takemoto L, Takehana M. Covalent change of major intrinsic polypeptide (MIP26K) of lens membrane during human senile cataractogenesis. Biochem Biophys Res Commun. 1986; 135:965–971. [PubMed: 2421726]
45. Do Ngoc L, Paroutaud P, Dunia I, Benedetti EL, Hoebeke J. Sequence analysis of peptide fragments from the intrinsic membrane protein of calf lens fibers MP26 and its natural maturation product MP22. FEBS Lett. 1985; 181:74–78. [PubMed: 3882455]
46. Schey KL, Fowler JG, Shearer TR, David LL. Modifications to rat lens major intrinsic protein in selenite-induced cataract. Invest Ophthalmol Vis Sci. 1999; 40:657–667. [PubMed: 10067969]
47. Kumari SS, Varadaraj K. Intact AQP0 Performs Cell-to-Cell Adhesion. Biochem Biophys Res Commun. 2009; 390:1034–1039. [PubMed: 19857466]
48. Kumari SS, Eswaramoorthy S, Mathias RT, Varadaraj K. Unique and analogous functions of aquaporin 0 for fiber cell architecture and ocular lens transparency. Biochim Biophys Acta. 2011; 1812:1089–1097. [PubMed: 21511033]
49. Varadaraj K, Kumari SS, Patil R, Wax MB, Mathias RT. Functional characterization of a human aquaporin 0 mutation that leads to a congenital dominant lens cataract. Exp Eye Res. 2008; 87:9–21. [PubMed: 18501347]
50. Kumari SS, Gandhi J, Mustehsan MH, Eren S, Varadaraj K. Functional characterization of an AQP0 missense mutation, R33C, that causes dominant congenital lens cataract, reveals impaired cell-to-cell adhesion. Exp Eye Res. 2013; 116:371–385. [PubMed: 24120416]
51. Smith BL, Agre P. Erythrocyte Mr 28,000 transmembrane protein exists as a multisubunit oligomer similar to channel proteins. J Biol Chem. 1991; 266:6407–6415. [PubMed: 2007592]
52. Buck TM, Wagner J, Grund S, Skach WR. A novel tripartite motif involved in aquaporin topogenesis, monomer folding and tetramerization. Nature Struct Mol Biol. 2007; 14:762–769. [PubMed: 17632520]

53. Yap AS, Brieher WM, Gumbiner BM. Molecular and functional analysis of cadherin-based adherens junctions. Annu Rev Cell Dev Biol. 1997; 13:119–146. [PubMed: 9442870]
54. Hiroaki Y, Tani K, Kamegawa A, Gyobu N, Nishikawa K, Suzuki H, Walz T, Sasaki S, Mitsuoka K, Kimura K, Mizoguchi A, Fujiyoshi AY. Implications of the aquaporin-4 structure on array formation and cell adhesion. J Mol Biol. 2006; 355:628–639. [PubMed: 16325200]
55. Chandy G, Zampighi GA, Kreman M, Hall JE. Comparison of the water transporting properties of MIP and AQP1. J Membr Biol. 1997; 159:29–39. [PubMed: 9309208]
56. Takemoto LJ. Quantitation of specific cleavage sites at the C-terminal region of alpha-A crystallin from human lenses of different age. Exp Eye Res. 1998; 66:263–266. [PubMed: 9533852]
57. Lund AL, Smith JB, Smith DL. Modifications of the water-insoluble human lens alpha-crystallins. Exp Eye Res. 1996; 63:661–672. [PubMed: 9068373]
58. Kistler J, Bullivant S. Protein processing in lens intercellular junctions: cleavage of MP70 to MP38. Invest Ophthalmol Vis Sci. 1987; 28:1687–1692. [PubMed: 3654141]
59. Lin JS, Fitzgerald S, Dong YM, Knight C, Donaldson P, Kistler J. Processing of the gap junction protein connexin50 in the ocular lens is accomplished by calpain. Eur J Cell Biol. 1997; 73:141–149. [PubMed: 9208227]
60. Lin JS, Eckert R, Kistler J, Donaldson P. Spatial differences in gap junction gating in the lens are a consequence of connexin cleavage. Eur J Cell Biol. 1998; 76:246–250. [PubMed: 9765054]
61. Tenbroek E, Arenson M, Jarvis L, Loius C. The distribution of the fiber cell intrinsic membrane proteins MP20 and connexin46 in the bovine lens. J Cell Sci. 1992; 103:245–257. [PubMed: 1331134]
62. Jacobs MD, Soeller C, Sisley AM, Cannell MB, Donaldson PJ. Gap junction processing and redistribution revealed by quantitative optical measurements of connexin46 epitopes in the lens. Invest Ophthalmol Vis Sci. 2004; 45:191–199. [PubMed: 14691173]
63. Wang Z, Obidike JE, Schey KL. Posttranslational modifications of the bovine lens beaded filament proteins filensin and CP49. Invest Ophthalmol Vis Sci. 2010; 51:1565–1574. [PubMed: 19875662]
64. Gonen T, Sliz P, Kistler J, Cheng Y, Walz T. Aquaporin-0 membrane junctions reveal the structure of a closed water pore. Nature. 2004; 429:193–197. [PubMed: 15141214]
65. Gonen T, Cheng YF, Sliz P, Hiroaki Y, Fujiyoshi Y, Harrison SC, Walz T. Lipid–protein interactions in double-layered two-dimensional AQPO crystals. Nature. 2005; 438:633–638. [PubMed: 16319884]
66. Harries WE, Akhavan D, Miercke LJ, Khademi S, Stroud RM. The channel architecture of aquaporin 0 at a 2.2-A resolution. Proc Natl Acad Sci USA. 2004; 101:14045–14050. [PubMed: 15377788]
67. Jensen M, Dror R, Xu H, Borhani D, Arkin I, Eastwood M, Shaw D. Dynamic control of slow water transport by aquaporin 0: implications for hydration and junction stability in the eye lens. Proc Natl Acad Sci USA. 2008; 105:14430–14435. [PubMed: 18787121]
68. Michea LF, de la Fuente M, Lagos N. Lens major intrinsic protein (MIP) promotes adhesion when reconstituted into large unilamellar liposomes. Biochemistry. 1994; 33:7663–7669. [PubMed: 8011633]
69. Michea LF, Andrinolo D, Ceppi H, Lagos N. Biochemical evidence for adhesion-promoting role of major intrinsic protein isolated from both normal and cataractous human lenses. Exp Eye Res. 1995; 61:293–301. [PubMed: 7556493]
70. Costello MJ, McIntosh TJ, Robertson JD. Membrane specializations in mammalian lens fiber cells: distribution of square arrays. Curr Eye Res. 1985; 4:1183–1201. [PubMed: 4075818]
71. Costello MJ, McIntosh TJ, Robertson JD. Distribution of gap junctions and square array junctions in the mammalian lens. Invest Ophthalmol Vis Sci. 1989; 30:975–989. [PubMed: 2722452]
72. Sweeney MH, Truscott RJ. An impediment to glutathione diffusion in older normal human lenses: a possible precondition for nuclear cataract. Exp Eye Res. 1998; 67:587–595. [PubMed: 9878221]
73. Moffat BA, Landman KA, Truscott RJ, Sweeney MH, Pope JM. Age-related changes in the kinetics of water transport in normal human lenses. Exp Eye Res. 1999; 69:663–669. [PubMed: 10620395]

74. Truscott RJ. Age-related nuclear cataract: a lens transport problem. Ophthalmic Res. 2000; 32:185–194. [PubMed: 10971179]
75. Zampighi G, Simon SA, Robertson JD, McIntosh TJ, Costello MJ. On the structural organization of isolated bovine lens fiber junctions. J Cell Biol. 1982; 93:175–189. [PubMed: 7068755]
76. Zampighi GA, Eskandari S, Hall JE, Zampighi L, Kreman M. Micro-domains of AQP0 in lens equatorial fibers. Exp Eye Res. 2002; 75:505–519. [PubMed: 12457863]
77. Ferreira-Cornwell MC, Veneziale RW, Grunwald GB, Menko AS. N-cadherin function is required for differentiation-dependent cytoskeletal reorganization in lens cells *in vitro*. Exp Cell Res. 2000; 256:237–247. [PubMed: 10739670]
78. Xu L, Overbeek PA, Reneker LW. Systematic analysis of E-, N- and P-cadherin expression in mouse eye development. Exp Eye Res. 2002; 74:753–760. [PubMed: 12126948]
79. Leonard M, Chan Y, Menko AS. Identification of a novel intermediate filament-linked N-cadherin/gamma-catenin complex involved in the establishment of the cytoarchitecture of differentiated lens fiber cells. Dev Biol. 2008; 319:298–308. [PubMed: 18514185]
80. Pontoriero GF, Smith AN, Miller LA, Radice GL, West-Mays JA, Lang RA. Co-operative roles for E-cadherin and N-cadherin during lens vesicle separation and lens epithelial cell survival. Dev Biol. 2009; 326:403–417. [PubMed: 18996109]
81. Maddala R, Chauhan BK, Walker C, Zheng Y, Robinson ML, Lang RA, Rao PV. Rac1 GTPase-deficient mouse lens exhibits defects in shape, suture formation, fiber cell migration and survival. Dev Biol. 2011; 360:30–43. [PubMed: 21945075]
82. Atreya PL, Barnes J, Katar M, Alcala J, Maisel H. N-cadherin of the human lens. Curr Eye Res. 1989:947–956. [PubMed: 2676356]
83. Costello MJ, Johnsen S, Metlapally S, Gilliland KO, Ramamurthy B, Krishna PV, Balasubramanian D. Ultrastructural analysis of damage to nuclear fiber cell membranes in advanced age-related cataracts from India. Exp Eye Res. 2008; 87:147–158. [PubMed: 18617164]
84. Kuszak, JR.; Costello, MJ. The Structure of the Vertebrate Lens. In: Lovicu, FJ.; Robinson, ML., editors. Development of the Ocular Lens. Cambridge University Press; Cambridge, UK: 2004. p. 71-118.
85. Lo WK, Harding CV. Square arrays and their role in ridge formation in human lens fibers. J Ultrastruct Res. 1984; 86:228–245. [PubMed: 6544861]
86. Lo WK, Biswas SK, Brako L, Shiels A, Gu S, Jiang JX. Aquaporin-0 targets interlocking domains to control the integrity and transparency of the eye lens. Invest Ophthalmol Vis Sci. 2014; 55:1202–1212. [PubMed: 24458158]
87. Bassnett S. On the mechanism of organelle degradation in the vertebrate lens. Exp Eye Res. 2009; 88:133–139. [PubMed: 18840431]
88. Taylor VL, al-Ghoul KJ, Lane CW, Davis VA, Kuszak JR, Costello MJ. Morphology of the normal human lens. Invest Ophthalmol Vis Sci. 1996; 37:1396–1410. [PubMed: 8641842]
89. Al-Ghoul KJ, Nordgren RK, Kuszak AJ, Freel CD, Costello MJ, Kuszak JR. Structural evidence of human nuclear fiber compaction as a function of ageing and cataractogenesis. Exp Eye Res. 2001; 72:199–214. [PubMed: 11180969]
90. Costello MJ, Mohamed A, Gilliland KO, Fowler WC, Johnsen S. Ultrastructural analysis of the human lens fiber cell remodeling zone and the initiation of cellular compaction. Exp Eye Res. 2013; 116:411–418. [PubMed: 24183661]
91. Wang Z, Schey KL. Aquaporin-0 interacts with the FERM domain of ezrin/radixin/moesin proteins in the ocular lens. Invest Ophthalmol Vis Sci. 2011; 52:5079–5087. [PubMed: 21642618]
92. Lindsey Rose KM, Gourdie RG, Prescott AR, Quinlan RA, Crouch RK, Schey KL. The C terminus of lens aquaporin 0 interacts with the cytoskeletal proteins filensin and CP49. Invest Ophthalmol Vis Sci. 2006; 47:1562–1570. [PubMed: 16565393]
93. Nakazawa Y, Oka M, Furuki K, Mitsuishi A, Nakashima E, Takehana M. The effect of the interaction between aquaporin 0 (AQP0) and the filensin tail region on AQP0 water permeability. Mol Vis. 2011; 17:3191–3199. [PubMed: 22194645]
94. Clark JI, Matsushima H, David LL, Clark JM. Lens cytoskeleton and transparency: a model. Eye (Lond). 1999; 13:417–424. [PubMed: 10627819]

95. Rao PV. The pulling, pushing and fusing of lens fibers: a role for Rho GTPases. Cell Adh Migr. 2008; 2:170–173. [PubMed: 19262112]
96. Rao PV, Maddala R. The role of the lens actin cytoskeleton in fiber cell elongation and differentiation. Semin Cell Dev Biol. 2006; 17:698–711. [PubMed: 17145190]
97. Gokhin DS, Nowak RB, Kim NE, Arnett EE, Chen AC, Sah RL, Clark JI, Fowler VM. Tmod1 and CP49 synergize to control the fiber cell geometry, transparency, and mechanical stiffness of the mouse lens. PLoS One. 2012; 7:e48734. [PubMed: 23144950]
98. Yu XS, Jiang JX. Interaction of major intrinsic protein (aquaporin-0) with fiber connexins in lens development. J Cell Sci. 2004; 117:871–880. [PubMed: 14762116]
99. Yu XS, Yin X, Lafer EM, Jiang JX. Developmental regulation of the direct interaction between the intracellular loop of connexin 45.6 and the C terminus of major intrinsic protein (aquaporin-0). J Biol Chem. 2005; 280:22081–22090. [PubMed: 15802270]
100. Liu BF, Liang JJ. Confocal fluorescence microscopy study of interaction between lens MIP26/AQP0 and crystallins in living cells. J Cell Biochem. 2008; 104:51–58. [PubMed: 18004741]
101. Gupta R, Asomugha CO, Srivastava OP. The common modification in alpha A-crystallin in the lens, N101D, is associated with increased opacity in a mouse model. J Biol Chem. 2011; 286:11579–11592. [PubMed: 21245144]
102. Fan J, Donovan AK, Ledee DR, Zelenka PS, Fariss RN, Chepelinsky AB. GammaE-crystallin recruitment to the plasma membrane by specific interaction between lens MIP/aquaporin-0 and gammaE-crystallin. Invest Ophthalmol Vis Sci. 2004; 45:863–871. [PubMed: 14985303]
103. Alcala, J.; Maisel, H. Biochemistry of lens plasma membrane and cytoskeleton. In: Maisel, H., editor. The Ocular Lens: Structure, Function and Pathology. Marcel Dekker; New York: 1985. p. 169-222.
104. Sandilands A, Prescott AR, Hutcheson AM, Quinlan RA, Casselman JT, FitzGerald PG. Filensin is proteolytically processed during lens fiber cell differentiation by multiple independent pathways. Eur J Cell Biol. 1995; 67:238–253. [PubMed: 7588880]
105. Blankenship TN, Hess JF, FitzGerald PG. Development- and differentiation-dependent reorganization of intermediate filaments in fiber cells. Invest Ophthalmol Vis Sci. 2001; 42:735–742. [PubMed: 11222535]
106. FitzGerald PG. Lens intermediate filaments. Exp Eye Res. 2009; 88:165–172. [PubMed: 19071112]
107. Oka M, Kudo H, Sugama N, Asami Y, Takehana M. The function of filensin and phakinin in lens transparency. Mol Vis. 2008; 14:815–822. [PubMed: 18449355]
108. Alizadeh A, Clark JI, Seeberger T, Hess J, Blankenship T, Spicer A, FitzGerald PG. Targeted genomic deletion of the lens-specific intermediate filament protein CP49. Invest Ophthalmol Vis Sci. 2002; 43:3722–3727. [PubMed: 12454043]
109. Alizadeh A, Clark JI, Seeberger T, Hess J, Blankenship T, FitzGerald PG. Targeted deletion of the lens fiber cell-specific intermediate filament protein filensin. Invest Ophthalmol Vis Sci. 2003; 44:5252–5258. [PubMed: 14638724]
110. Alizadeh A, Clark JI, Seeberger T, Hess J, Blankenship T, FitzGerald PG. Characterization of a mutation in the lens-specific CP49 in the 129 strain of mouse. Invest Ophthalmol Vis Sci. 2004; 45:884–891. [PubMed: 14985306]
111. Aimon S, Callan-Jones A, Berthaud A, Pinot M, Toombes GE, Bassereau P. Membrane shape modulates transmembrane protein distribution. Dev Cell. 2014; 28:212–218. [PubMed: 24480645]
112. Aponte-Santamaría C, Briones R, Schenk AD, Walz T, de Groot BL. Molecular driving forces defining lipid positions around aquaporin-0. Proc Natl Acad Sci U S A. 2012; 109:9887–9892. [PubMed: 22679286]
113. Shi Y, Barton K, De Maria A, Petrash JM, Shiels A, Bassnett S. The stratified syncytium of the vertebrate lens. J Cell Sci. 2009; 122:1607–1615. [PubMed: 19401333]
114. Kopylova LV, Cherepanov IV, Snytnikova OA, Rumyantseva YV, Kolosova NG, Tsentalovich YP, Sagdeev RZ. Age-related changes in the water-soluble lens protein composition of Wistar and accelerated-senescence OXYS rats. Mol Vis 2011. 2011; 17:1457–1467.

Highlights

- N- and proximal end of C- terminus of AQP0 are important for protein trafficking
- Water permeability and adhesion are not affected by AQP0 N- or C- terminal cleavage
- N- and C-terminal truncation of AQP0 appears to be a fiber cell maturation event
- AQP0 N- and C-terminal truncations may aid in the compaction of cytosolic proteins
- AQP0 may assist in adjusting lens refractive index to prevent spherical aberration

Figure 1A

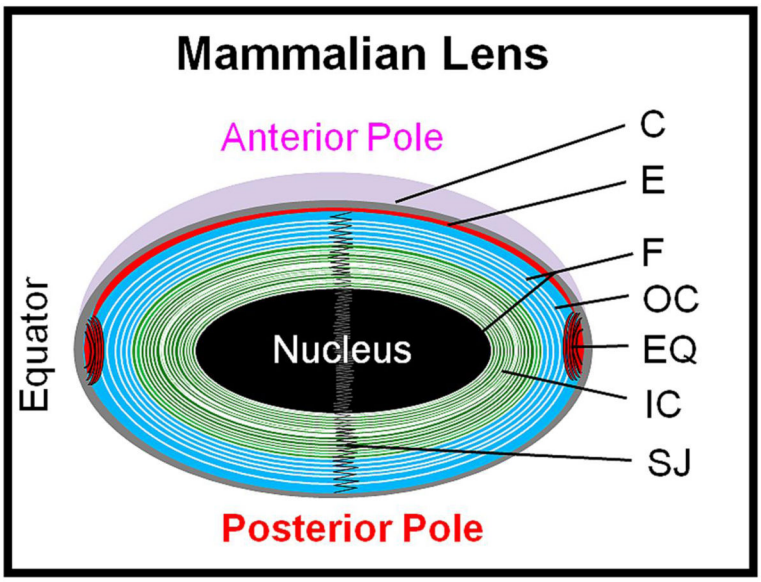

Figure 1B

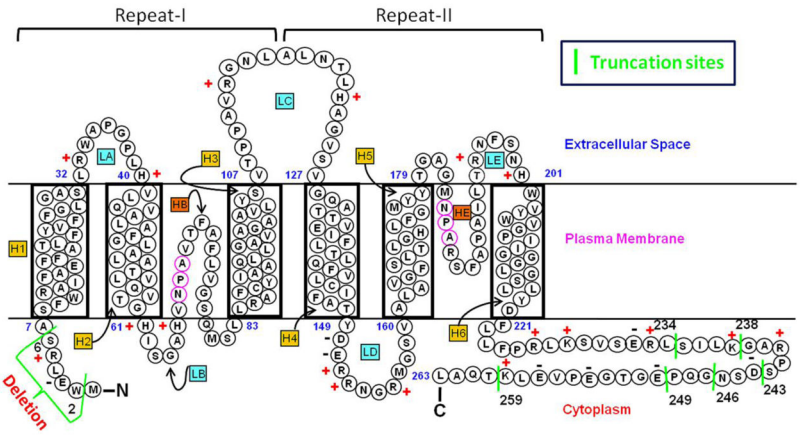

Fig. 1.

(A). Schematic (not to scale) representation of the adult mammalian lens. C, capsule; E, anterior epithelial cells; EQ, equatorial epithelial cells; F, fiber cells; IC, inner cortex; OC, outer cortex; SJ, fiber cell suture junction. (**B)** Schematic representation of human AQP0 showing selected natural post-translational deletion/truncations. AQP0 monomer structure shows folds, helix assignment, and location at the membrane. Transmembrane-spanning alpha helices are shown as H1–H6 and loops as LA–LE. The two aquapore lining helices are shown as HB and HE. Highly conserved NPA motifs in HB and HE that line the water pore of aquaporin are denoted as magenta circles. N, amino terminus; C, carboxyl terminus. '+' and '−' represent amino acid charges in the extracellular and cytoplasmic domains. Truncation sites are marked as green vertical lines with the corresponding number of the amino acid nearby.

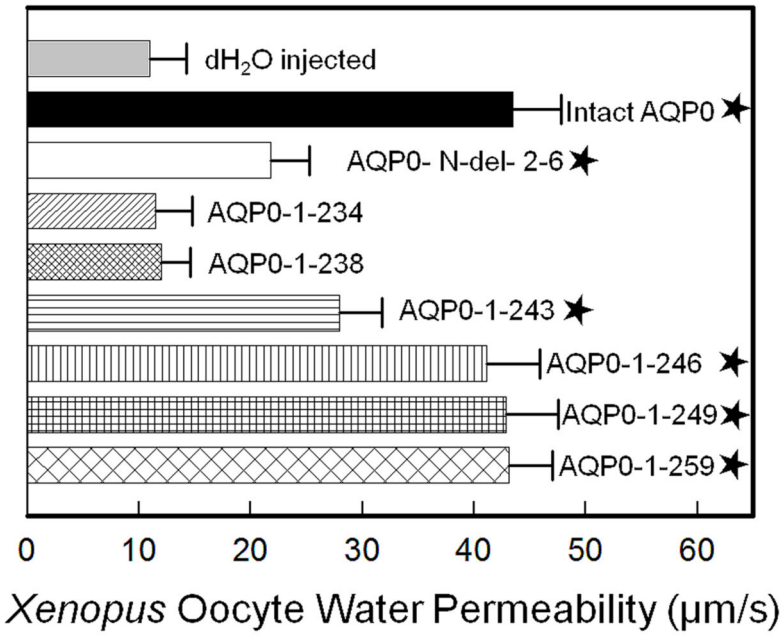

Fig. 2.

Membrane Pw of *Xenopus laevis* oocytes injected with distilled water, 25 ng/oocyte cRNA of intact AQP0 or N- or C- terminal truncated AQP0. Initial rate of swelling was estimated by placing each oocyte in a hypotonic solution. Membrane Pw was calculated as described in the "Materials and Methods' section. Average oocyte membrane Pw of five swelling assays for each sample is shown (each assay with 10 oocytes; (mean ± SD)). Asterisk represents the degree of significance in comparison to dH_2O injected control, $P < 0.001$.

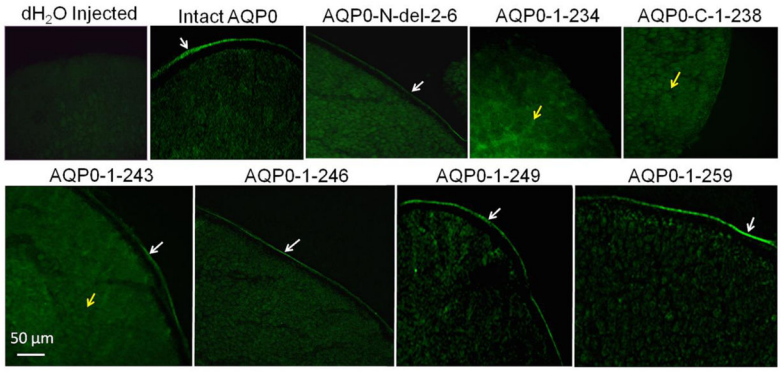

Fig. 3.

Expression of intact AQP0, and N- or C- terminal truncated AQP0 tagged with EGFP in *Xenopus laevis* oocytes. Immunostaining of cryosections of oocytes injected with distilled water or cRNA of intact AQP0 or N- or C- terminal truncated AQP0 visualized by epifluorescence microscopy. White arrows - protein localization at the plasma membrane; Yellow arrows - protein localization in the cytoplasm.

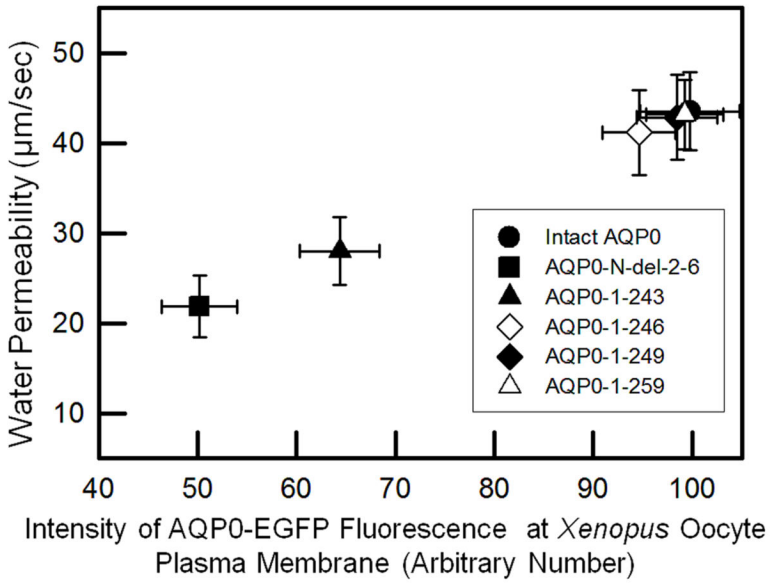

Fig. 4.

Correlation between protein expression of intact AQP0 or N- or C- terminal truncated AQP0 at the oocyte plasma membrane and oocyte plasma membrane Pw.

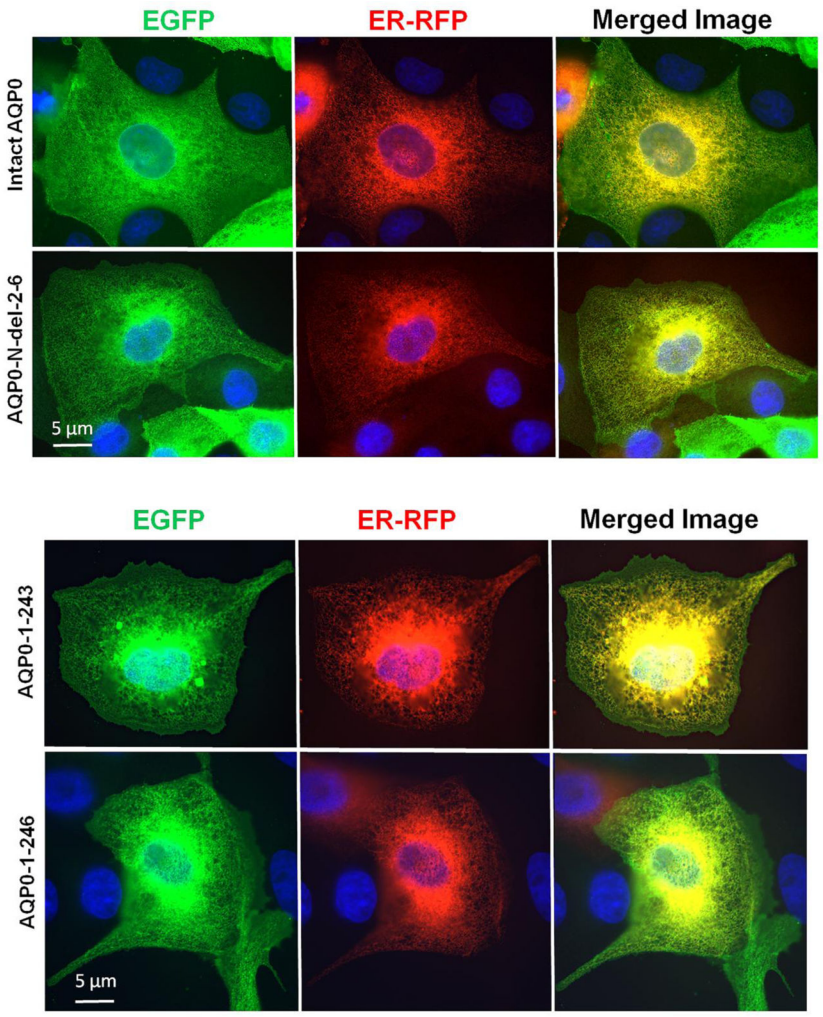

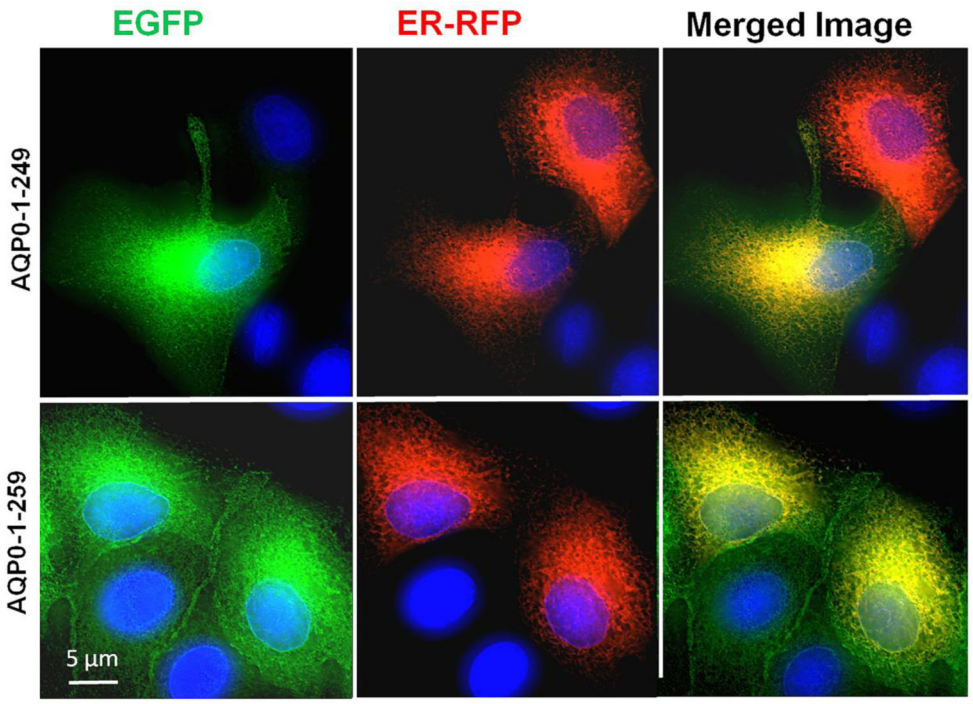

Fig. 5.

Localization and colocalization of intact AQP0-EGFP, or N- or C- terminal truncated AQP0-EGFP with organelle light ER-RFP, in MDCK cells. Coexpressing cells were viewed under an EGFP fluorescent filter and the same cells were viewed under Texas Red fluorescent filter; both images were merged by overlaying to see protein localization at ER and plasma membrane; Yellow color is due to the colocalization of the respective protein (green) in the ER along with the organelle light (red). The green fluorescence seen at the periphery of the images indicates plasma membrane localization of AQP0. Nuclei are stained with DAPI (blue).

Fig. 6A.

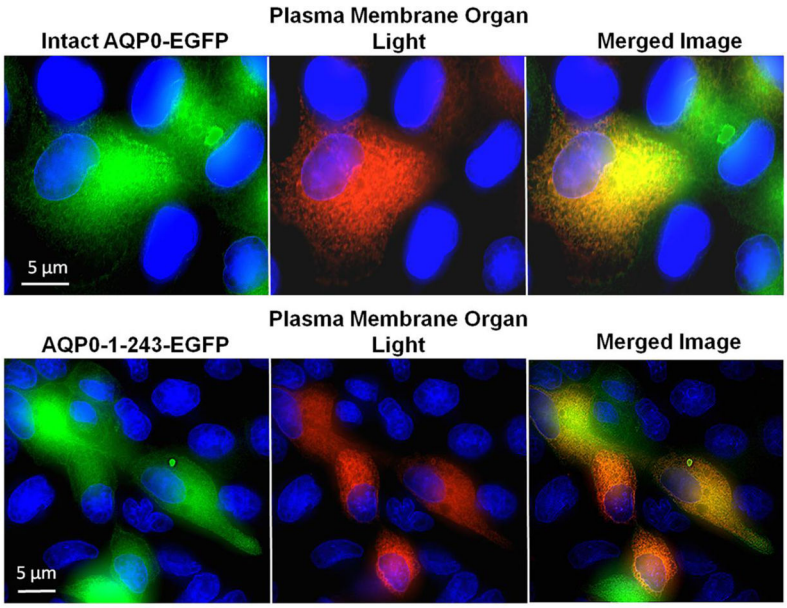

Fig. 6B

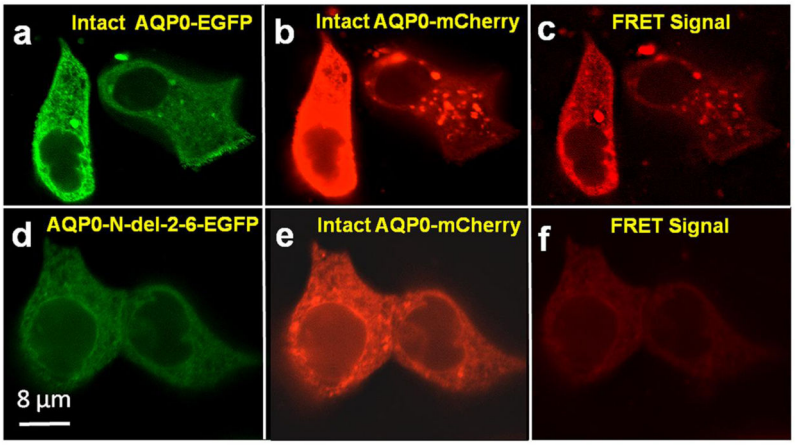

Fig. 6B

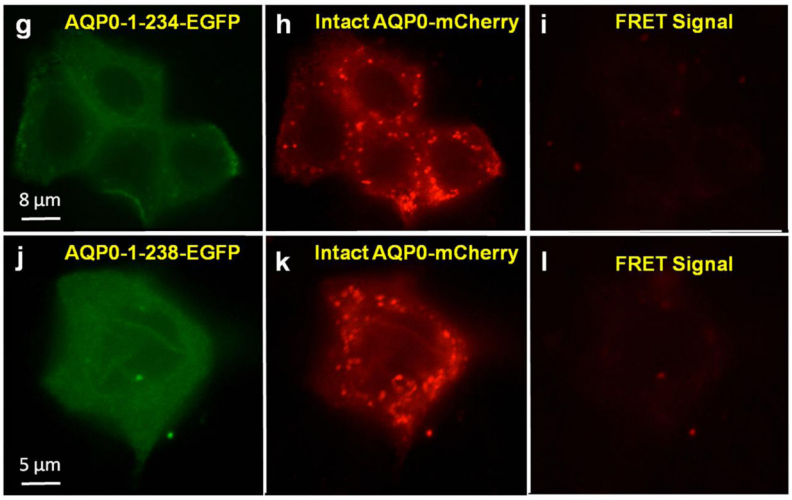

Fig. 6B

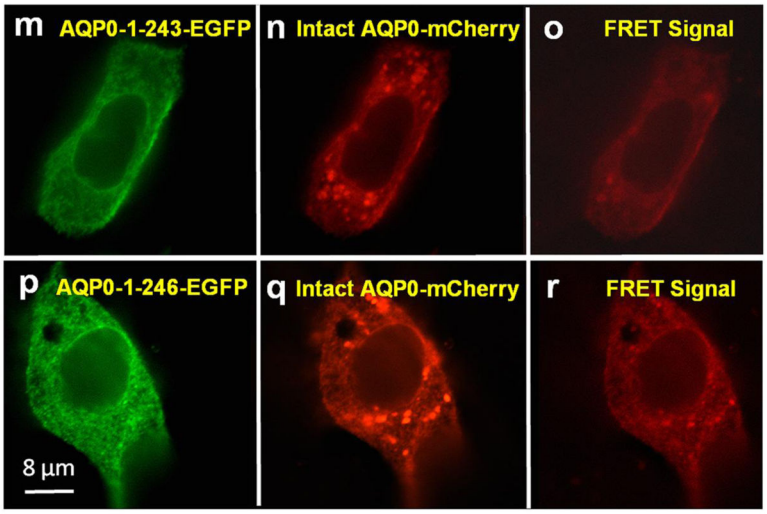

Fig. 6B

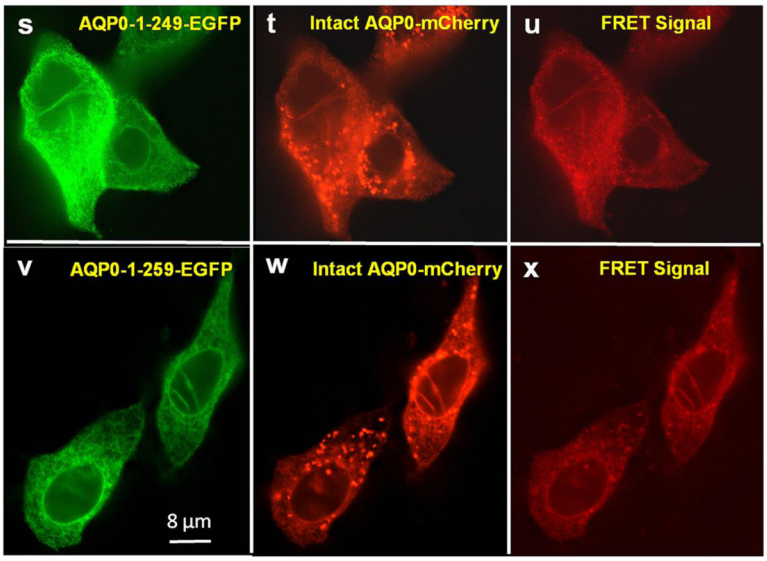

Fig. 6.

A. Colocalization of intact AQP0-EGFP or AQP0-1-243-EGFP and plasma membrane organ light. Coexpressing cells were viewed under an EGFP fluorescent filter and the same cells were viewed under Texas Red fluorescent filter; both images were merged by overlaying to see protein localization at the plasma membrane. **B.** Protein colocalization using FRET signal intensity. **(a–x)** Forster Resonance Energy Transfer studies in MDCK cells cotransfected with intact AQP0-EGFP and intact AQP0-mCherry (**a–c**) or N-, or C- terminal truncated AQP0-EGFP and intact AQP0-mCherry (**d–x**). **(a, d, g, j, m, p, s, v)** cells excited at 488 nm and emission recorded at 507 nm; **(b, e, h, k, n, q, t, w)** cells excited at 587 nm and emission recorded at 610 nm; **(c, f, i, l, o, r, u, x)** cells excited at 470 nm and emission recorded at 640 nm fluorescence due to FRET; **(c, f, i, l, o, r, u, x)** fluorescence indicating colocalization of intact AQP0-EGFP and intact AQP0-mCherry or N-, and C- terminal truncated AQP0-EGFP and intact AQP0-mCherry proteins in the same oligomer or within 100Å. Nuclei are stained with DAPI (blue).

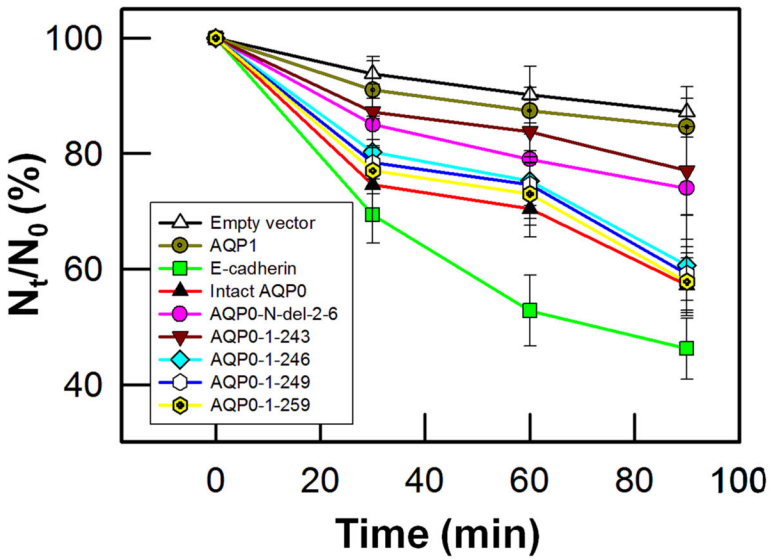

Fig. 7.

Cell aggregation assay using rotary gyratory shaker. Cell aggregation exhibited by adhesion-deficient L-cells expressing untagged empty vector, AQP1, E-cadherin, intact AQP0, and N- or C- terminal truncated AQP0 in relation to incubation time. (N_t - total number of particles at time 't' of incubation; N_0 - initial number of particles).

Figure 8A

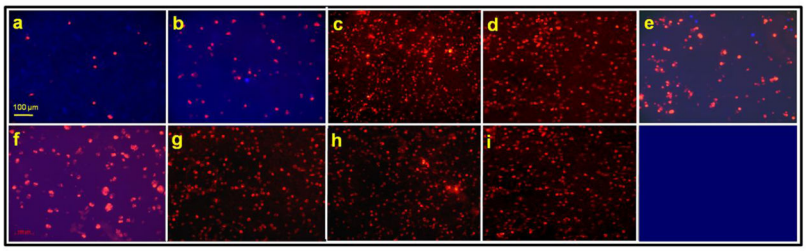

Fig. 8B

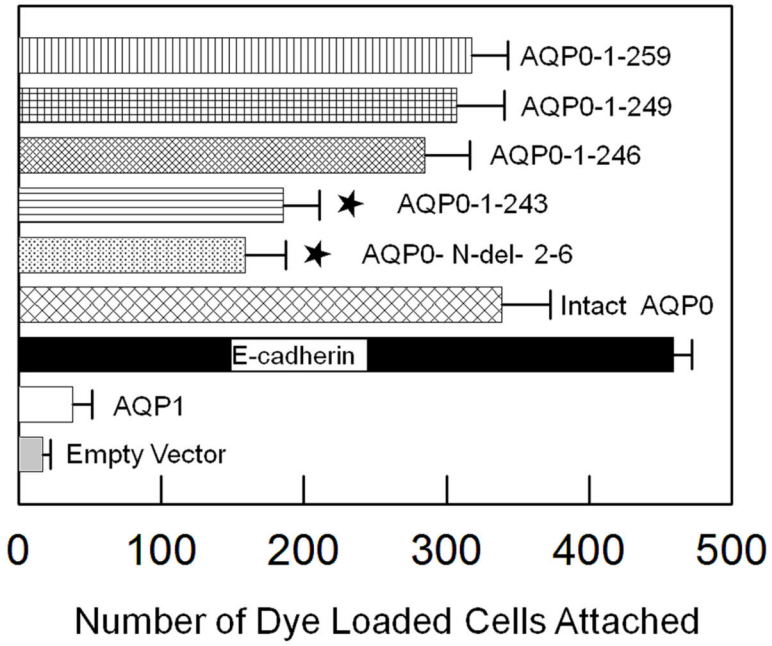

Figure 8C

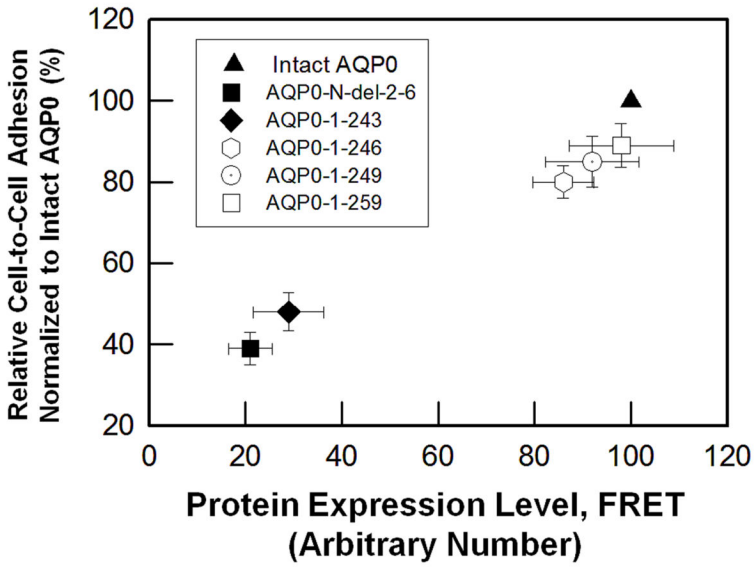

Fig. 8.

(A). Cell-to-cell adhesion (CTCA) assay using an epifluorescent microscope. Over a monolayer of L-cells expressing untagged empty vector (a), AQP1 (b), E-cadherin (c), intact AQP0 (d) or N- and C- terminal truncated AQP0 (AQP0-N-del-2-6 (e), AQP0-1-243 (f), AQP0-1-246 (g), AQP0-1-249 (h), AQP0-1-259 (i)), corresponding cells loaded with CellTracker Red were plated. At the end of the procedure described in the 'Materials and methods' section, the cells were imaged under an epifluorescent microscope. Cells/ aggregates were counted and plotted. **(B).** Bar graph showing the extent of CTCA exhibited after 60 min of incubation by the samples tested using the fluorescence assay. *AQP0-N-del-2-6 and AQP0-1-243 exhibited significantly low ($P < 0.001$) CTCA compared to intact AQP0. **(C).** Correlation between protein expression at the oocyte plasma membrane by intact AQP0 or N-, and C- terminal truncated AQP0 and the extent of CTCA exerted by each sample.

Fig. 9A

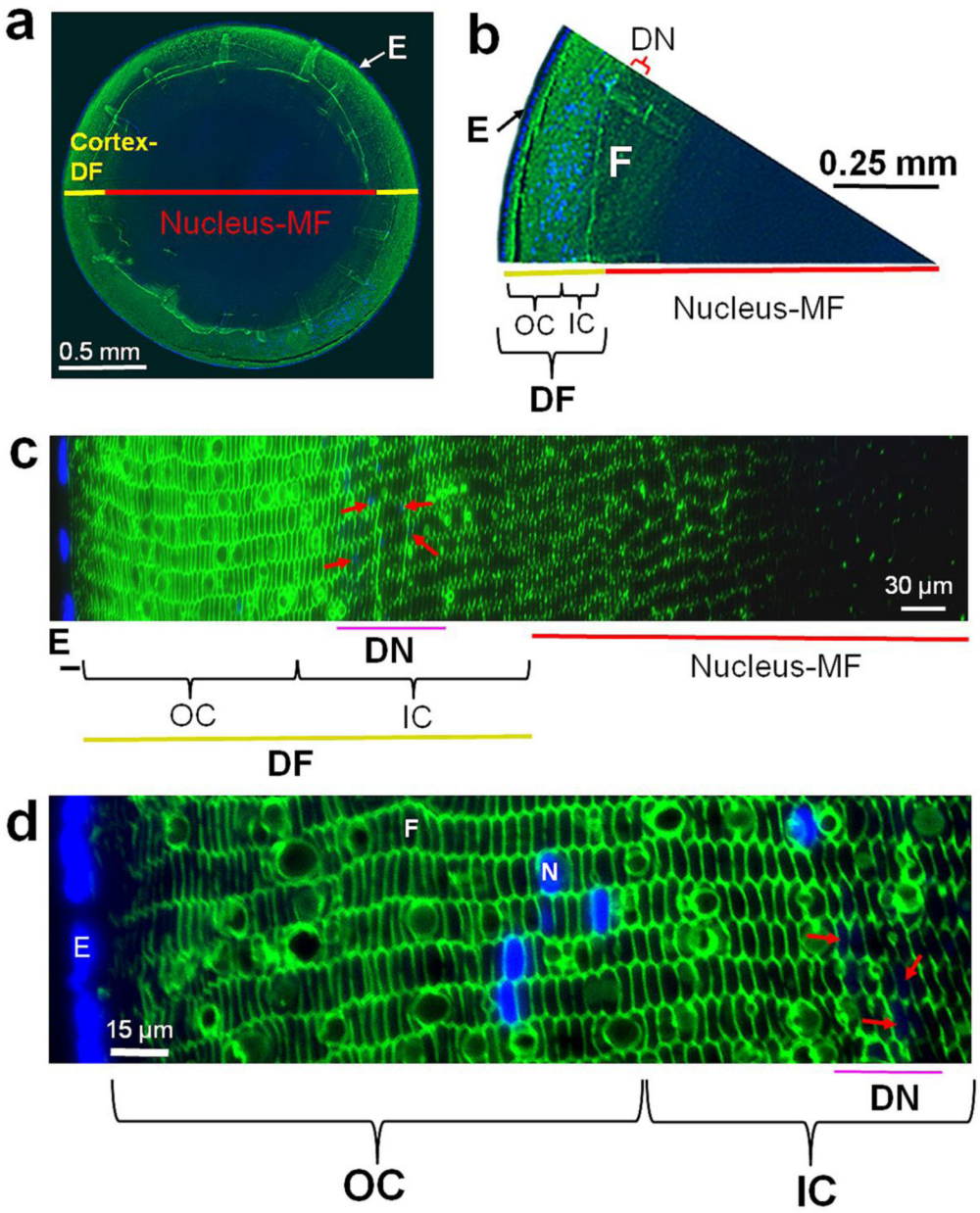

Fig. 9B

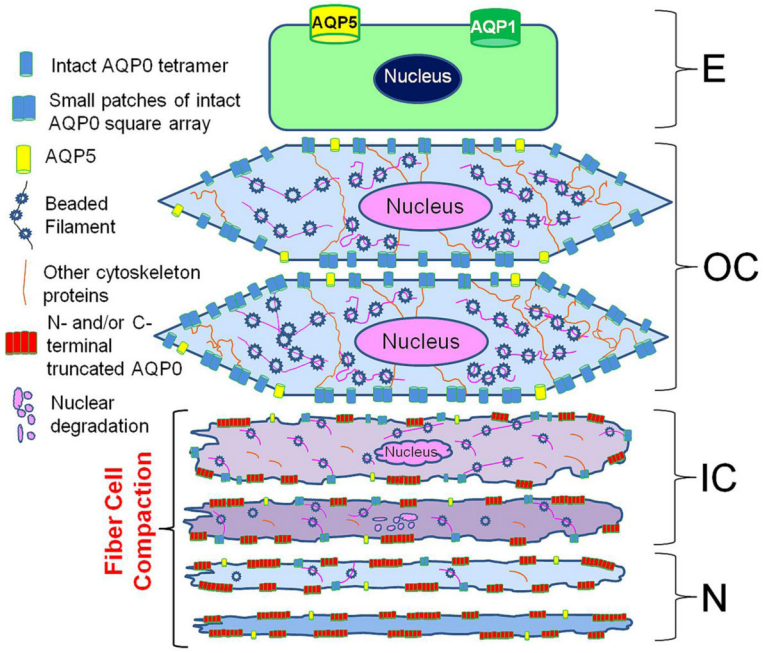

Fig. 9C

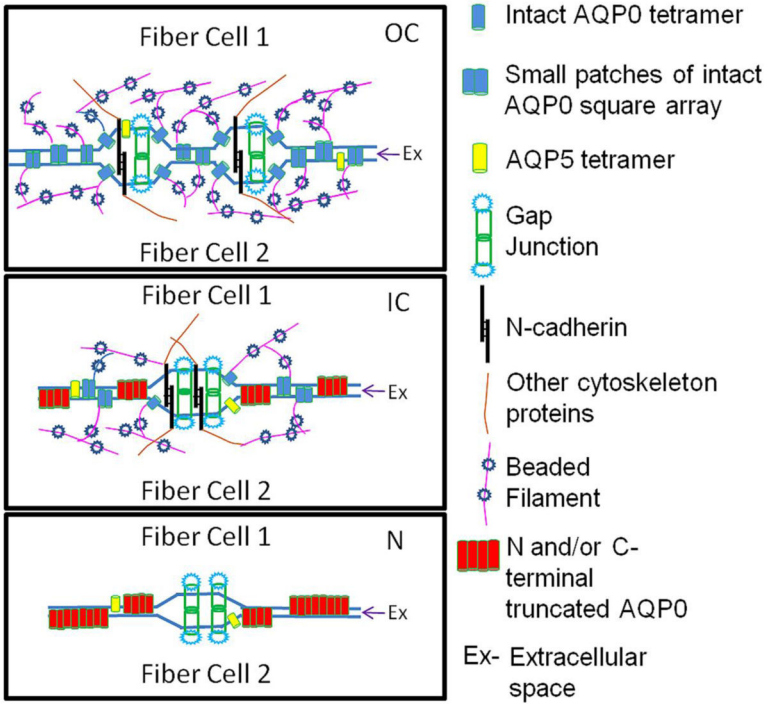

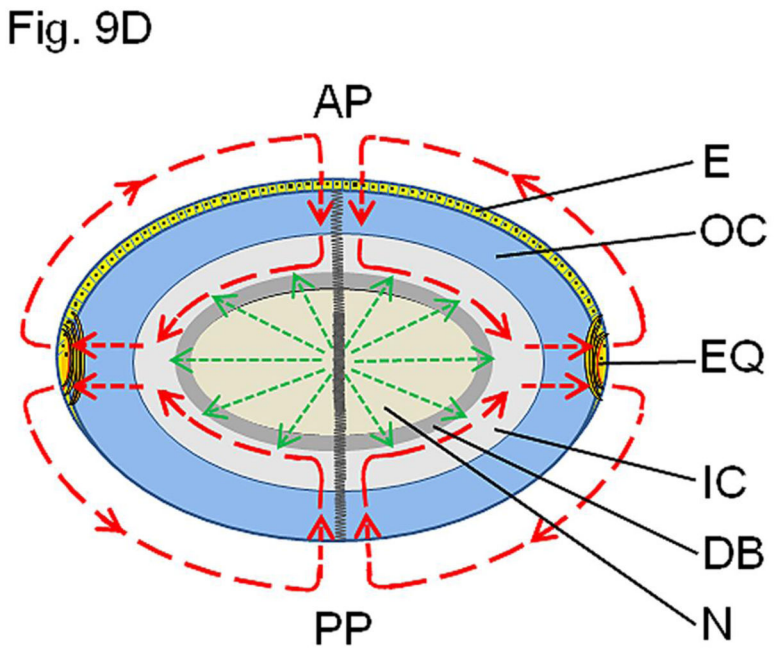

Fig. 9.

(A). Immunocytochemistry of 4-month-old wild type mouse lens to show patterns of anti-AQP0 antibody binding. The antibody was raised against a 17 amino acid (AA247-263) synthetic peptide from the cytoplasmic carboxyl terminal domain of human AQP0 (Chemicon, Temecula, CA). **(a, b)** Lens cross sections close to the equatorial region at low magnification; **(c,d)** Magnified portions from the lens cross-sectional image (a). The C-terminal specific anti-AQP0 antibody bound (green) to lens outer and inner cortical fiber cells which contain the differentiating and differentiated secondary fiber cells, respectively. Low levels of antibody binding occurred to the outermost layers of lens nuclear fiber cells; the antibody did not bind to much of the lens nuclear fiber cells suggesting most of the C-terminal AQP0 epitopes had been lost due to the natural post-translational truncation which had been reported by mass spectrometry studies [32, 33,37], probably for fiber cell compaction [89,90]. During fiber cell maturation, cellular organelles like nucleus disintegrate (shown in red arrows) to reduce light scattering and to enable cell compaction for adjusting the lens refractive index. The blue spots represent cell nuclei stained with DAPI. E-Epithelial cells; F- fiber cells; DF- Differentiating fiber cells; DN- denucleation zone; IC- Inner cortex; MF- Mature fiber cells; N-Nucleus; OC- Outer cortex. **(B).** Schematic model showing the morphology of the differentiating and differentiated fiber cells in the lens and the changes with reference to post-translational N- and C-terminal end truncations of AQP0. In the outer cortex (OC), fiber cells maintain a flattened hexagonal shape (Fig.9A) with nearly uniform distribution of small plaques of regular square arrays of AQP0 tetramers whose N- and C-terminal ends interact with cytoplasmic proteins like lens-specific beaded filaments (shown in the model), actins, crystallins and plasma membrane proteins. Lens fiber cell-specific beaded filament cytoskeleton formed by filensin and CP49 may influence cortical fiber cell shape and uniform distribution of AQP0. In the inner cortex (IC), fiber cell rearrangements occur through remodeling in order to reduce light scattering and to adjust the refractive index of the constantly growing lens. Fiber cell nuclei and other

cellular organelles disintegrate and disappear at the end of remodeling. The mature fiber cells at the inner cortex and nucleus (N) become undulated, losing the hexagonal shape. Loss of the N- and C-terminal ends of AQP0 and the consequent loss of tethering with other proteins probably frees AQP0 and leads to tetramer aggregation at the plasma membrane in the inner cortex and nucleus (in red) forming large patches of AQP0 square arrays which possibly pair with the protein-free lipid membrane bilayers to develop new thin junctions which are asymmetric. This event probably increases the fiber cell-to-fiber cell adhesion and reduces extracellular space and water gradually to increase the refractive index in the mature fiber cells. The fiber cells with undulated membranes in the inner cortex and nuclear regions undergo compaction process and become terminally differentiated mature nuclear fiber cells. During compaction, redistribution of plasma membrane proteins as well as removal of cytosolic water content (dehydration) takes place. The beaded filament proteins and other cytoskeletal proteins are degraded gradually from inner cortex to nucleus during fiber cell maturation, remodeling and compaction. **(C)** Diagram detailing the formation of large patches of square array thin junctions of AQP0 between the plasma membranes of two adjacent fiber cells for CTCA. In the outer cortex **(OC)** intact AQP0 (in light blue) interact with fiber cell-specific cytoskeletal beaded filament proteins (shown in the diagram), actins and crystallins with its N- and C-terminal ends and get nearly uniformly distributed throughout the plasma membrane. Plasma membranes of adjacent fiber cells form thin junctions with small patches of AQP0 square arrays, adhesion junctions with N-cadherin and gap junctions with connexins resulting in a mixture of large and small extracellular space which retains more water and probably helps to maintain the characteristic low refractive index of the outer cortex. In the mature fiber cells of inner cortex **(IC)** and Nucleus **(N)**, N-cadherin is lost gradually resulting in the loss of adhesion junctions altogether in the nucleus. In the mature fiber cells of inner cortex (IC) and Nucleus (N) a gradual loss of N- and C-terminal ends of AQP0 which interacts with the cytoskeletal and other proteins lead to the loss of its uniform distribution. This enables AQP0 to migrate and form tetramer aggregates (in red) to form large square array patches with asymmetric thin junctions which help to gradually reduce extracellular space and water to increase the refractive index characteristic of lens interior to aid in focusing of objects on to the retina. N-cadherin is absent in the nucleus. The large patches of square arrays with thin junctions push the gap junctions to their periphery as shown in atomic microscopy images [11–13]. E-epithelium. **(D)** Schematic diagram to show the development of the diffusion barrier in the inner cortex (gray circle around the nucleus) and solute and water removal fluxes from the interior of the lens. During fiber cell compaction, reduction in extracellular space and removal of water takes place probably creating a solute and water flux from the lens nucleus to the inner cortex (green arrows) to adjust the lens refractive index in mammalian lens. In the outer cortex, the solute and water enter the lens fiber cells by passive diffusion (red arrows) at the poles and exit at the equator [8]. We postulate that the water and solutes coming out of the nucleus (green arrows) meet the exit flow [8] of solutes and water at the inner cortex and this region which restricts solutes and water entry into the nuclear region could be the area generally recognized as the diffusion barrier (DB). Delivery of solutes and water to the lens core may be very minimal through sutures because the lens inner cortex and nucleus eliminate free water along with solutes by dehydration process to adjust the refractive index. We hypothesize that the outflow of water (green arrows) from the inner cortex and nuclear

region joins the water flow from the outer cortex ([8] red arrows) and exit at the equator. AP, anterior pole; E, anterior epithelial cells; EQ, equator, OC, outer cortex; IC inner cortex; DB, diffusion barrier; N, nucleus. PP, posterior pole.

Table 1

Plasma membrane water permeability of *Xenopus laevis* oocytes injected with the cRNA of intact or N- or C-terminal truncated AQPO

cRNA-injected	Membrane water permeability (μm/s)
Distilled water injected (control)	11.0± 3.2
Intact AQP0	43.5 ± 4.3
AQP0-N-del-2-6	21.8 ± 3.4
AQP0-1-234	11.5 ± 3.3
AQP0-1-238	12.0 ± 2.6
AQP0-1-243	28.0 ± 3.7
AQP0-1-246	41.2 ± 4.7
AQP0-1-249	42.8 ± 4.7
AQP0-1-259	43.2 ± 3.9